Crowdedness, Mispricing, Crashes, and Spikes

Boulis Maher Ibrahim[1]
Heriot Watt University,
Centre for Social and Economic Data Analytics (CSEDA)

Iordanis Angelos Kalaitzoglou[2]
Audencia Business School,
Department of Finance, MATES

Abstract

This study proposes "reflexive crowdedness" as a mechanism through which order flow can become toxic at ultra-high frequencies (UHFs). We show that crowdedness, a coordination problem that arises from the inability of traders to accurately gauge competition, leads to significant mispricing in UHFs in the form of liquidity costs. This mispricing propagates through (reflexive) feedback loops between liquidity variations and price components and can accumulate rapidly when high-speed traders engage. We develop an empirical framework to examine this mechanism in UHF trading. Empirical results on trades of Dow 30 stocks show that reflexive crowdedness triggers speculative algorithmic trading and is a key driver of order flow toxicity and market instability at high frequencies. Further, we develop a new UHF measure of crowdedness and find it predicts various UHF phenomena, including flash crashes and spikes, more reliably than price volatility and the Volume Synchronised Probability of Informed Trading (VPIN). We propose important recommendations for investors, market operators, and regulators.

JEL classifications : C41; C58; G15

Keywords: Crowdedness; Microstructure; Arbitrage capacity; Overreaction; High frequency trading (HFT)

---

[1] Edinburgh Business School, Accounting, Economics and Finance Department, CSEDA, Riccarton, Edinburgh, Scotland, UK, EH14 4AS. Email: b.m.ibrahim@hw.ac.uk, Tel: +443560 Teams.
[2] Corresponding Author. Audencia Business School, Department of Finance, Research Center: (MA)rkets (TE)chnology and (S)ociety. 8 Route de la Joneliere, 44312, Cedex 3, Nantes, France. Email: ikalaitsoglou@audencia.com, Tel: +33(0)240378102.

1. Introduction

We propose a mechanism we call "reflexive crowdedness" through which order flow becomes increasingly toxic at ultra-high frequencies (UHFs). This mechanism combines *crowdedness*, a coordination problem that arises when traders cannot accurately gauge competition, and *reflexivity*, a price dynamic based on feedback loops. A trader identifying an arbitrage opportunity cannot condition trading on competition due to uncertainty about the number of competitors and their capacity to conduct arbitrage. Consequently, this trader might transact at prices that overshoot or undershoot their fundamental values. We hypothesise that mispricing from this coordination problem (crowdedness) induces noise in trading signals that triggers speculative trading. This noise can propagate through feedback loops between arbitrage capacity and the information and liquidity costs that other traders estimate from trading signals. These feedback loops (reflexivity) fuel further speculative trading that accumulates rapidly at UHFs due to high-speed opportunistic algorithmic traders (algos).[3] These conditions can nudge the market into a self-propagating liquidity state, or "liquidity spiral," requiring intervention or substantial price movements to restore equilibrium. Thus, reflexive crowdedness can render order flow toxic, causing traders to unknowingly provide liquidity at a loss. In this paper, we introduce an empirical framework to investigate this mechanism in UHFs, demonstrating that it can lead to various UHF extreme phenomena, including flash crashes and spikes.

Short-lived, extreme price events are increasingly common at UHFs. Johnson et al. (2013) documented 18,520 such events from 2006 to 2011, and our analysis found 1,472 similar events in Dow 30 stocks in 2019. Although the causes are debated, algos are often implicated due to

[3] At UHFs, speed becomes the "token of information" (O'Hara, 2015). The literature recognises two types of algos: agency and opportunistic (Hagströmer and Nordén, 2013; Li et al., 2021). Agency algos engage in market making as liquidity providers, facilitating trading and diffusing information by interacting with informed agents such as fund managers (Hendershott et al., 2015). Opportunistic algos are liquidity takers who rely on speed and engage in UHF strategies, such as low-latency arbitrage, directional speculation, and one-side market making (O'Hara, 2015; Boehmer et al., 2018). Both types extract price-relevant information from entropic trading signals and, in a sense, free ride on fundamental information (Yadav, 2015).

trading at speeds that outpace human attention.[4] However, speed alone may not drive these events. Algos can support market liquidity (e.g., Linton et al., 2011; Hasbrouck and Saar, 2013; Brogaard et al., 2014), but their reliance on speed and liquidity-related information rather than firm fundamentals (O'Hara, 2015) means they can both supply and deplete liquidity quickly (Yao and Ye, 2018). Thus, liquidity bouts may coincide with increased algo presence. However, in efficient markets, mere liquidity bouts should not lead to the significant decline in market quality seen in extreme events (Johnson et al., 2013). Breckenfelder (2024) shows that speculative trading rises and market quality declines when high-frequency traders compete rather than when their numbers increase. This suggests that while algo presence and speed matter, they may not be the main drivers of speculative competition during extreme events. The implication is that the overreliance of algos on speed and non-fundamental information may induce noise in trading signals that fuels speculative competition. Yet, the literature does not explain why or when competition in UHFs becomes speculative, leading to extreme events. We argue that extreme events stem from toxic order flow that turns competition speculative. This motivates our focus on crowdedness as the mechanism that renders order flow toxic. Our analysis shows that crowdedness from uncertainty in arbitrage capacity imposes significant liquidity costs, causing liquidity suppliers to unknowingly provide liquidity at a loss. Thus, crowdedness can drive the toxicity of order flow that triggers speculative competition.

The reflexivity aspect of our mechanism is motived by the fact that while crowdedness can cause persistent mispricing (Stein, 2009), it may be insufficient to trigger extreme price events at UHFs. The zero-profit condition of efficient markets implies a balance between overreaction and underreaction (Fama, 1998). However, UHF extreme events involve rapid, sustained mispricing in one direction, often requiring intervention like circuit breakers or spikes in the

---

[4] The U.S. Commodity Futures Trading Commission (CFTC) and the U.S Securities and Exchange Commission (SEC) (2010) report on the 6 May 2010 flash crash, for example, reinforces this perspective by noting that "prices were moving so fast, fundamental traders and arbitrageurs were either unable or unwilling to supply enough [buy-side] liquidity" (p. 4). Although the report suggests speed as the main factor, it left it unclear how the speed of trading rendered traders unable or unwilling to supply liquidity during the crash.

bid-ask spread. Algos may explain the speed (Li et al., 2021), but sustained mispricing suggests a clustering mechanism. If reflexive loops feed the noise from crowded trading signals into prices, then clusters may form in order flow toxicity, leading to liquidity spirals. We develop a microstructure pricing model where information and liquidity price components vary with *expected* arbitrage capacity, modelled as an autoregressive moving average (ARMA) process. Formulating arbitrage capacity as the product of this ARMA process and random noise captures both persistence and clustering. This results in an asymmetric information price component positively affected by persistence in arbitrage capacity (liquidity) and a liquidity price component negatively affected by this persistence. These opposing loops allow the model to capture market conditions dominated by either information concerns (normal trading) or liquidity fears (extreme events). Thus, reflexivity can account for the rapid onset of liquidity spirals leading to extreme price movements like flash crashes or spikes.[5]

The concept of crowdedness was first explored in the asset pricing literature. Stein (2009), for example, considers two types of agents: "newswatchers" who underreact to information and arbitrageurs who attempt to profit from this underreaction. Through simulations, Stein shows that uncertainty in the *number* of arbitrageurs can lead to persistent mispricing in long-term strategies unanchored to fundamentals, such as momentum strategies and carry trades. Abreu and Brunnermeier (2003) investigate a similar effect from traders' inability to synchronise their trades due to uncertainty in the *timing* of trades. Our framework goes beyond these and other related asset pricing studies in several ways. First, unlike most asset pricing literature focusing on arbitrages across assets or maturities, our framework deals with

[5] This reflexivity mechanism is distinctly different from the liquidity spirals of Brunnermeier and Pederson (2009) that relate to trader funding constraints and the magnifying effect of leverage with no funding constraints studied in Stein (2009), among others. Brunnermeier and Pedersen (2009) propose two liquidity spirals. A *margin spiral* emerges if traders' margins are increasing in illiquidity, and a *loss spiral* arises if speculators hold large initial positions that are negatively correlated with customer demand shocks. A funding shock decreases market liquidity, leading to higher margins (margin spiral) and speculator losses on their initial positions forcing more sales and price drops (loss spiral). By contrast, our framework neither assumes funding constraints nor leverage. Magnification occurs through sequential clustering of mispricing arising from uncertainty in arbitrage capacity.

sequential information arbitrage in the same asset. Second, while Stein (2009) and others consider two types of agents, we model competitive interactions among three types: informed, uninformed, and discretionary liquidity traders (Kyle, 1985; Admati and Pfleiderer, 1988), with algos as a subset of discretionary liquidity traders. Third, our study is the first to model arbitrage capacity holistically in three dimensions: the *number* of each agent type, their *capital*, and the *speed* at which they can apply it. This accounts for both the intensity and capacity (capital and speed) of agent types to compete for arbitrage opportunities. Fourth, unlike Stein (2009) who considers random fundamentals, we model evolving fundamentals conditioned on noisy order flow and *expected* arbitrage capacity, accounting for changing private information and interactions between liquidity (arbitrage capacity) and information costs. Fifth, our empirical framework is not confined to simple long-term strategies that are unanchored to fundamentals, as in Stein (2009), but considers every trade as a potential arbitrage opportunity. This requires a new trade-by-trade measure of crowdedness which we develop in this paper.

Our study also relates to the microstructure literature where mispricing is typically attributed to liquidity costs, information costs, or speculative trading. For instance, Chordia and Subrahmanyam (2004) focus on liquidity factors like autocorrelated order imbalances from large order splitting and market maker inventory constraints. Conversely, Sarkar and Schwartz (2009) attribute mispricing to asymmetric information among agents, leading to one-sided trading, and differential information due to heterogeneous beliefs, leading to two-sided trading. Additionally, Tkatch and Kandel (2004) explore the interaction between information and liquidity in causing shifts in demands for immediacy. Finally, Breckenfelder (2024) finds market quality deteriorates when high-frequency traders trade speculatively. This literature acknowledges the price impact of information and liquidity-related effects. However, there is no study on crowdedness and mispricing at UHF. Existing models do not capture crowdedness at UHFs, being either theoretical with frictionless market assumptions or empirical but focused on lower frequencies. Prior theoretical approaches use partial equilibrium models, limited sequential information models, or pricing that does not fully account for all trading costs or changes in fundamentals. Empirical approaches are limited by their adaptation to lower-frequency trading issues, such as calendar or discrete time, experimental market setups, and simple long-term trading strategies or two-agent classification. They do not explain what triggers the accumulation of speculative competitiveness among UHF traders and the toxicity of order flow at certain times. Our mechanism addresses these issues directly.

Our approach goes beyond the previous literature in several ways. First, it employs a pricing mechanism enforcing a zero-profit equilibrium condition, with violations reflected as liquidity costs. To extract these costs, we need a trade indicator model tailored to UHFs. We enhance Madhavan et al.'s (1997) asymmetric information microstructure model in three ways.[6] The first enhancement allows agent responses to information and liquidity costs to vary with *expected* arbitrage capacity. Thus, price formation is designed to be regret-free of *expected* arbitrage capacity, in addition to the standard microstructure factors of private information, public information, liquidity costs, and price discreteness. The second enhancement is the identification of agent types by modelling arrival rates as point processes, inferring three distinct agent types from trading intensities or hazard functions of their volume interactions with the market (Ibrahim and Kalaitzoglou, 2016). The third enhancement accounts for differential information in trade size (volume) and speed (duration).[7] Mispricing is then calculated by filtering out the effect of evolving fundamentals from price changes. Thus, our mispricing measure focuses solely on liquidity costs, providing a more relevant metric of order flow toxicity than price volatility or Easley et al.'s (2011a, b) VPIN, which use total price changes. Second, besides accounting for all three dimensions of arbitrage capacity and three types of rational competitive agents, our model considers both asymmetric and differential information (Sarkar and Schwartz, 2009) as competition drivers. Third, the model accounts for

[6] See Madhavan (2000) for a review of trade indicator models.
[7] Madhavan et al.'s (1997) model ignores this information by assuming equally spaced trades of unit size.

the autocorrelation in returns and volatility often linked to market inefficiencies or behavioural biases like herding. These autocorrelations are induced by the persistence in the ARMA process assumed for expected arbitrage capacity. Finally, the model incorporates reflexivity and changing fundamentals by dynamically updating agent responses to new information and changes in liquidity costs on a trade-by-trade basis, thereby operating in event time rather than calendar time. Our estimation results show significant clustering in arbitrage capacity that identifies three distinct agents and coupled with the reflexive loops differentially affects their responses to information and liquidity costs. In such a dynamic, regret-free setup with rational agents, the prior literature predicts the disappearance of the crowdedness effect (see Stein, 2009). Thus, our framework is more holistic, rigorous, and appropriate than previous studies for examining crowdedness in UHFs, constituting our first contribution to the literature.

Our second contribution is the empirical evidence of crowdedness in UHFs. In efficient markets, mispricing should average symmetrically around zero (Fama, 1998). However, our analysis shows that mispricing and mispricing risk in Dow 30 trades increase asymmetrically with the size of *surprise* in arbitrage capacity (SAC), especially during faster-than-expected trading or for low-liquidity stocks. Additionally, on good news days, mispricing is greater in slow trading conditions. These asymmetries confirm the presence of crowdedness in UHF trading, even when using an elaborate pricing model to estimate mispricing.

Our third contribution is twofold. We introduce a new UHF measure of trade crowdedness based on the rate of mispricing per unit of SAC and assess its predictive power on several UHF phenomena. These phenomena include extreme price events, sudden demands for immediacy (impatience), price runs (herding or behavioural biases), sudden increases in the bid-ask spread and price volatility, and the intensity of algorithmic and institutional trading. First, we evaluate whether crowdedness in individual trades predicts these phenomena over different time horizons. Second, we compare the predictive power of an interval-based version of our measure with that of price volatility and VPIN for UHF extreme price events. The results show that crowdedness significantly predicts these phenomena up to 150 transactions ahead, acts as a trigger to speculative algo trading, and is a stronger and more stable predictor of flash crashes and spikes than VPIN and price volatility. This provides an ex-ante measure of order flow toxicity and the market's propensity to enter a liquidity spiral.

In the remainder of this paper, Section 2 develops our pricing model and mispricing measure, Section 3 presents the data, Section 4 analyses crowdedness and its predictive power on UHF phenomena using a new measure of crowdedness, Section 5 discusses implications of the results on investors, operators, and regulators, and Section 6 concludes.

2. Structural pricing and a mispricing measure

Consider a risky security with an evolving fundamental value $\tilde{v}_i$, which trades through a trading mechanism where bid-ask quote setting is ex-post rational. We extend Madhavan et al.'s (1997) pricing model to incorporate variations in expected liquidity of the next trade in both the traders' revisions in beliefs about fundamental value and the impact of liquidity costs on the change in prices. The revision in beliefs ($\Delta\mu_i$) and the change in price (Δp_i) from trade *i*-1 to trade *i* are:

$$\mu_i - \mu_{i-1} \equiv \Delta\mu_i = \theta_i(q_i - E[q_i|q_{i-1}]) + \varepsilon_i, \tag{1}$$

$$p_i - p_{i-1} \equiv \Delta p_i = \Delta\mu_i + \Delta\varphi_i q_i + \Delta\xi_i = \theta_i(q_i - \rho q_{i-1}) + \Delta\varphi_i q_i + \varepsilon_i + \Delta\xi_i, \tag{2}$$

where $\mu_i \equiv E[\tilde{v}_i|H_i]$ is the post-trade expectation of the fundamental value $\tilde{v}_i$ of the risky security at *event/trade* time *i* given the available information set H_i; q_i is an order flow variable that takes a value of +1 (-1) if trade *i* is buyer (seller) initiated, and is assumed to follow a simple Markov process with ρ being its first order autocorrelation; the term $(q_i - E[q_i|q_{i-1}])$, where $E[q_i|q_{i-1}] = \rho q_{i-1}$, is the surprise in order flow, considered to be a noisy signal of private information; θ_i is a time-varying asymmetric information parameter, or the agent's response to the private information indicated by the surprise in order flow; φ_i is a time-varying agent's price response to liquidity; $\varphi_i q_i$ is signed liquidity cost; ε_i is public information; and $\xi_i \sim iid(0)$ are errors due to time-varying returns or price discreteness.[8]

Unlike Madhavan et al.'s (1997) model in which θ and φ are constants, this model differentiates the effects of *anticipated* and *unanticipated* arbitrage capacity by specifying the price responses to information and liquidity, θ_i and φ_i, respectively, as functions of *expected* arbitrage capacity and the presence of each agent type according to the following dynamics:

$$\theta_i = \theta_1 + \left(\theta_2^{uninf} I_i^{uninf} + \theta_2^{DL} I_i^{DL} + \theta_2^{inf} I_i^{inf}\right)\Theta_\iota^{-1}, \tag{3}$$

$$\varphi_\iota = \varphi_1 + \left(\varphi_2^{uninf} I_i^{uninf} + \varphi_2^{DL} I_i^{DL} + \varphi_2^{inf} I_i^{inf}\right)\Theta_\iota^{-1}, \tag{4}$$

where θ_1, φ_1, θ_2^l and φ_2^l, $l = \{$*uninformed, discretionary liquidity (DL), informed*$\}$ are parameters to be estimated, Θ_ι^{-1} is the capital and timing of the arbitrage capacity that is *expected* to be applied to trade *i*, and I_i^l is a set of dummy variables that prospectively classifies trade i as informed, DL, or uninformed. We next describe how Θ_ι^{-1} and I_i^l are determined.

In an intraday context, we conjecture that two main dimensions of the arbitrage capacity *applied* by traders are primarily reflected in the size (volume) and timing (duration) of their trades. We consider the *rate per unit time* of the capital employed as a single measure that combines both the size and time dimensions of arbitrage capacity that is applied to a trade. This measure is the rate of transacted volume, or the ratio of trade volume to trade duration, v_i/d_i. The reciprocal of this measure is volume-weighted duration, d_i/v_i, or the time taken to trade one contract. First, we diurnally (seasonally) adjust the raw duration d_i and call it x_i. We then transform x_i into volume-weighted duration $S_i = x_i K(u_i)$ using the time deformation (stretching and compacting) factor $K(u_i) = exp\left(-u_i/2\right)$, where $u_i = (v_i - \bar{v})/\sigma_v$ is normalised volume. The volume-transformed variable, S_i, is our explicit measure of *trading intensity*, or the inverse of applied arbitrage capacity, defined as the waiting (deformed) time

[8] In Madhavan et al. (1997) the parameters θ and φ are constant and common across agents and trades. Hence, their model assumes a representative agent and ignores variations in liquidity and changing responses to information. It also ignores information in trade size and speed as it assumes equally spaced trades of unit volume.

that a single contract takes to be traded.[9] Thus, by modelling trading intensity we simultaneously model the inverse of arbitrage capacity that is actually applied to trade i. S_i is a mark(volume)-weighted temporal point process, and we model it by the following Smooth Transition Mixture of Weibull Autocorrelated Conditional Volume Weighted Duration (STM-ACVWD) specification:

$$S_i = \Theta_i \eta_i \tag{5}$$

$$\Theta_i = \omega + \sum_{j=1}^{m} a_j S_{i-j} + \sum_{p=1}^{q} \beta_p \Theta_{i-p} \tag{6}$$

where Θ_i is the conditional *expected* trading intensity, or the reciprocal of *anticipated* arbitrage capacity that features in Equations (3) and (4); $\eta_i = S_i/\Theta_i$ is *unexpected* trading intensity or the reciprocal of *unanticipated* arbitrage capacity that is applied to trade *i*; and ω, a, β are parameter coefficients. Note from Equation (5) that the arbitrage capacity S_i applied to trade i is a noisy signal, with multiplicative noise, η_i, and Equations (5) and (6) describe how its signal-to-noise ratio is modelled. The conditional density function of the errors is assumed to be a smooth transition mixture of Weibull distributions in three regimes of trading intensity that identify the presence of uninformed, DL, and informed agents through variations in the hazard function of volume-weighted durations (Appendix B). A decreasing hazard indicates an acceleration of trading fuelled by the arrival of private information, which signals informed trading (resembling the "newswatchers" of Stein, 2009). An increasing hazard indicates an increasing probability of trading over time, which is consistent with the actions of arbitrageurs (trend chasers or discretionary liquidity traders) who need to extract an information signal first. Finally, a flat hazard indicates a continuation of the current level of liquidity that is in line with the assumed random rate of arrival of uninformed trading. The integral of the hazard function

[9] Note that this is a discrete measure of the instantaneous rate of transacted volume. It is a granular measure in the sense that it is a rate per unit of time, rather than an interval measure over a pre-specified ad-hoc interval of time (as PIN and VPIN are), and hence it avoids the uncertainty and controversy over volume bin determination in calculations of VPIN (see Andersen and Bondarenko, 2014a, b). Budish et al.'s (2023) suggestion of "Flow" or batch trading would regulate this trading intensity measure, and hence arbitrage capacity in the market.

over Δt in each of these three cases provides the count of informed, DL, and uninformed traders: I_i^{inf}, I_i^{DL}, and I_i^{uninf} that feature in Equations (3) and (4) (see Section B4 in Appendix B). Consequently, I_i^l refers to the expected presence of each agent type in a way that is consistent with the *anticipated number* of each type of player in the market. This accounts for the third dimension of arbitrage capacity that relates to the intensity of the presence of agents.

Equations (2) – (6) describe an advanced pricing model where quote setting and price formation satisfy zero-profit conditions, as all trading costs are accounted for through the full dissection of price changes. This price change is structured to be conditional on anticipated arbitrage capacity, the expected number of each of three types of players that may act on any arbitrage opportunity, the sign of the next trade, and public and private information.[10] Further, the point process modelling of the arrival rate of volume shares features with Filimonov et al.'s (2015) modelling of Hawkes processes used to measure the degree of endogeneity in self-exciting processes arising from feedback loops. In our model, the autocorrelation in Equation (6), which captures clustering in expected arbitrage capacity, is equivalent to a self-exciting Hawkes process and serves as the mechanism by which liquidity spirals can occur. The feedback loops (reflexivity) arise from two opposing liquidity effects: a positive effect in θ_i and a negative effect in φ_ι, because higher liquidity increases information costs (θ_i) but decreases liquidity costs (φ_ι). Furthermore, the model incorporates two *noisy* signals: private information and arbitrage capacity. Finally, it focuses on trades rather than orders but generates the best quotes that the market ought to set for the *next* trade. Hence, it imbeds regret-free estimates of the best bid and offer (BBO). These are limit orders, but their quotes are inferred from the model coefficients estimated from trade data. This approach has the advantage that the spread reflects the cost of "commitments" to trade, rather than contaminations from order

[10] Ibrahim and Kalaitzoglou (2016), who do not analyse overreaction and underreaction, report that a similar version of the model explains around 65% of the level of returns, 62% of the variance of returns, and 85% to nearly 100% of the GARCH effect in returns. It is, therefore, a reasonable contender for modelling price changes.

book manipulations such as those that can arise from order cancelations. Therefore, the focus is on trades rather than orders to capture the actual capital committed and applied to arbitrage opportunities. While we do not analyse order book depth beyond the BBO, our model considers both limit orders, through quote setting for the next trade, and market orders that resulted in previous trades, which are the limit orders that filled.

Given the above setup, we can now provide a measure of overreaction and underreaction. A natural measure of mispricing in a multi-period setup is the degree to which revisions in prices (Δp_i) deviate from revisions in beliefs ($\Delta \mu_i$). From Equations (1) and (2), this is:

$$\Delta p_i - \Delta \mu_i = \Delta \varphi_i q_i + \Delta \xi_i. \quad (7)$$

Conditional on the pricing model used, this is a function of changes in signed liquidity costs ($\Delta \varphi_i q_i$) and in price discreteness ($\Delta \xi_i$) since the previous trade, *i* – 1. Positive (negative) values for buy (sell) trades indicate overshooting or overreaction, and negative (positive) values for buy (sell) trades indicate undershooting or underreaction relative to revisions in fundamentals. Note that Equation (7) clearly indicates that changes in our model's mispricing are primarily due to variations in liquidity costs driven by changes in *anticipated* arbitrage capacity (in φ_i), which is the main cost relevant to liquidity traders. Importantly, this measure filters out the effect of evolving fundamentals (i.e., $\theta_i(q_i - E[q_i|q_{i-1}]) + \varepsilon_i$), including their dynamic interaction with the liquidity or trading intensity expected for the *next* trade (through θ_i).[11]

The unconditional mean of this mispricing measure is zero, which satisfies the equilibrium condition that, on average, prices reflect changes in beliefs due to private and public information, anticipated arbitrage capacity, the relative presence of players, signed liquidity costs, and price discreteness.[12] Accordingly, as signed liquidity costs and price discreteness

[11] Note that $\Delta \xi_i$ in Equation (7) is dropped in calculations for two reasons. First, it represents changes in price discreteness from one transaction to the next and this is likely to be zero on average within *SAC* bins, especially for the Dow 30 stocks. Second, only the variance of ξ_i can be estimated, which, being a constant, is safely excluded from tests of asymmetries of overreaction and underreaction based on averages over subsequent transactions.

[12] The unconditional variance is a function of ϕ_1, ϕ_2, the unconditional mean (constant), and the square of the ACVWD process, Θ. The conditional mean is time varying and is a function of ϕ_1, ϕ_2, ρ, q_{i-1}, ξ_{i-1}, and the

vary from one transaction to the next, overreaction or under-reaction too will vary as a function of changes in *anticipated* arbitrage capacity. However, if Equation (6) is an adequate description of expected trading intensity (in θ_i and φ_i), and since $\xi_i \sim iid(0)$, then overreaction or underreaction should be distributed *symmetrically* around the average of zero. Any mispricing arising from *surprises* in arbitrage capacity, therefore, should appear as liquidity cost effects distributed symmetrically around zero. Consequently, one should expect symmetry around zero in plots of the mispricing of Equation (7) against *unexpected* trading intensity η_i, which is also *unanticipated* arbitrage capacity (i.e., an impulse response function of Equation (7)). Thus, random unanticipated arbitrage capacity should have no bearing on average mispricing, which should be zero in an efficient (regret-free) market with an equilibrium adjusting mechanism. Henceforth, such plots, and associated tests, form the main tools of our investigation into the link between unanticipated arbitrage capacity and mispricing.

Note that in a balanced and efficient market, other forms of symmetry should also be expected. In particular, the conditional mean of our mispricing measure is:

$$(\rho - 1)\varphi_1 q_{i-1} + \sum_l \varphi_2^l I_i^l q_{i-1}(\rho\Theta_i - \Theta_{i-1}) - \xi_{i-1}, \tag{8}$$

with time-varying elements: q_{i-1}, ξ_{i-1}, and the change in Θ from *i* – 1 to *i*. Since this is a function of changes in (the inverse of) anticipated arbitrage capacity, the average overreaction given by the model should follow a roughly similar shape to the shock response function of the ACVWD model (see Fernandes and Grammig, 2006), and be symmetrically distributed across buy and sell transactions, since q_{i-1} is equally likely to be +1 (buy) or -1 (sell).

Another symmetry that should be expected relates to realisations of the type of news. If good and bad news are equally likely, then mispricing should also be symmetric across news types. Finally, since unexpected trading intensity η is *i.d.* with a mean of 1, and the shock response function of the ACVWD is symmetric across similarly sized realisations of η around

change in Θ from *i* – 1 to *i*. The conditional variance is time varying and is a function of ϕ_1, ϕ_2, ρ, and the conditional mean and square of Θ, which contain the variance (risk) of *unanticipated* arbitrage capacity, σ_η^2.

1, then mispricing should also be symmetric around $\eta = 1$. Our tests of crowdedness in Section 4.2 focus on detecting asymmetries in this impulse response function.

Besides the level of mispricing, we also analyse mispricing risk, or the *uncertainty* in overreaction and underreaction. The conditional variance of our mispricing measure is

$$(1-\rho^2)[\varphi_1^2 + 2\boldsymbol{\varphi_2}\varphi_1\Theta_i + (\boldsymbol{\varphi_2}\Theta_i)^2] + \sigma_{\xi_i}^2, \tag{9}$$

where $\boldsymbol{\varphi_2} = \sum_l \varphi_2^l I_i^l$, and the only time-varying element is the (inverse of) anticipated arbitrage capacity Θ_i. Hence, the conditional variance should also be symmetric around positive and negative realisations of unanticipated arbitrage capacity (η) of equal magnitude. Thus, both the level and the uncertainty of mispricing should be symmetric across *slower*- and *faster*-than-anticipated market conditions (i.e., $\eta > 1$ and $\eta < 1$, respectively, which also are positive and negative shocks in applied arbitrage capacity). A final type of asymmetry that we consider can arise from liquidity variations across stocks. Accordingly, we also analyse stocks by liquidity.

3. Data

We consider all transactions and national best quote revisions on the constituent stocks of the Dow 30 index from 2 January 2019 to 6 December 2019 traded on the following exchanges: AMEX, ARCA, BATS, BATS Y, CSE, EDGA, EDGX, FINRA, IEX, NASDAQ, NSE, and NYSE. The data is provided by Algoseek and presented in detail in the online Appendix.

We extract the time stamp in microseconds, the price in \$, and the volume in number of contracts of each recorded transaction and national best quote revision. The trade initiation variable is constructed using the tick rule of Harris (1989).[13] All observations outside the normal trading hours and the first transaction of each day, which aggregates the volume of the pre-opening auction, are omitted. Trades with identical time stamp, price, and direction are considered as one segmented trade and their volume is aggregated as if they were one trade.

[13] This is based on prices. Results using the alternative Ellis et al. (2000) tick rule are available upon request.

Duration is calculated as the time between consecutive trades in microseconds. We then add 1 sec. to all observations for computational reasons and diurnally adjust duration as in Engle and Russell (1998) to filter out seasonality. Trades outside the 0.01st–99.99th percentiles of price change and the 99.99th percentile of volume are filtered out as outliers. These adjustments result in a panel dataset of 230,084,293 filtered transactions on 30 stocks over 236 days. Panel A of Table 1 presents descriptive statistics of the sample return (R=Δp_i), volume (Q), and duration (D). Average return is near zero, average volume is 205.8 contracts, and average diurnally adjusted duration is 0.9 sec., but values vary considerably across stocks and range from -52.66 to 52.65 cents for returns, 1 to 88,000 contracts for volume, and 0 to 4,500 sec. for duration.

We further classify stocks by relative cross-sectional liquidity levels based on the total volume of trade. Stocks with a traded volume higher than the average across all stocks over the sample period are classified as High-Liquidity. The remaining stocks are classified as Low-Liquidity. The column entitled "HLiq" in Table A.1 in the online Appendix A shows that this method results in 11 out of the 30 stocks being classified as relatively highly liquid.

We also classify the trading days for each stock by the type of news into positive, no, and negative news days. This is initially conducted based on the distribution of trading imbalance. For each stock day, we calculate the daily volume trading imbalance as the difference between the daily buy volume and the daily sell volume. Next, we calculate the average of the absolute value of this imbalance over days for each stock. A stock day is classified as one of good (bad) news if the absolute imbalance for that day is higher (lower) than the daily average for that stock. A stock day is classified as having no news if the absolute imbalance for that day falls within the range of plus and minus the daily average. The values in the last 3 columns of Table A.1 show considerable variation across stocks in their classification of trading days. On average across stocks, 23% of days are classified as good news days, 62% as no news days, and 15% as bad news days. We also check robustness using an alternative news classification based on social media attention and sentiment (see Tables C.8 and C.9 in online Appendix C).

Therefore, the sample appears representative of a wide range of trading activity and price behaviour, even though the stocks are relatively highly liquid, being Dow 30 constituents.

4. Results and analyses

A summary of the estimation results of the arbitrage capacity model (Equations 5 and 6) and the pricing model (Equations 2 to 4) is presented in Panel B of Table 1. Detailed estimation results and full accompanying discussion are in the online Appendix B. We proceed here with the analysis of mispricing and start by testing for crowdedness.

We calculate a prospective measure of the average overreaction and underreaction from Equation (7) across the 5, 15, and 25 transactions following each trade i, which we refer to as *AOU*5, *AOU*15, and *AOU*25, respectively. This measure represents the predictive effect of *unanticipated* arbitrage capacity realised for trade i on *subsequent*, rather than contemporaneous, mispricing. We also calculate the inverse of unanticipated arbitrage capacity η_i of each trade i, but for graphical purposes we do so in additive form as $\Theta_i - S_i$, which is centred around zero, rather than the ratio S_i/Θ_i, which is centred around one. Henceforth, this measure is called the *SAC* (Surprise in Arbitrage Capacity). Positive *SAC* values indicate higher applied capacity than expected, or larger and faster trades than expected, and negative values indicate lower applied capacity than expected, or smaller and slower trades than expected.

Panel A of Table 1 presents summary statistics of *AOU* across stocks, and Tables A.2 and A.3 in the online Appendix A present more detail for each stock. These tables show that the mean and median *AOU* values for all stocks are close to zero. This generally supports the joint hypothesis that the pricing model is adequate, in the sense that it reflects changes in beliefs about fundamental values in price changes, and that the market is balanced, in the sense that it does not overreact more than it underreacts, *on average* (Fama, 1998). The standard deviation of *AOU* ranges from 0.17 to 3.11 across stocks, and decreases with longer windows, indicating that mispricing risk diminishes with the number of future transactions. This is also the case for each stock (see online Appendix A). Skewness ranges from -0.92 to near zero, and excess kurtosis ranges from -0.02 to 66.2 across stocks. These values suggest that while the average mispricing is zero, the distribution of mispricing may be asymmetric at high frequency. Such potential asymmetries are central to our analysis and are examined in detail below, considering the relative liquidity of a stock and the type of news.[14]

4.1. Asymmetries in mispricing

Graph 1 in Table 1 plots *AOU*15 over equally spaced *SAC* bins for high liquidity stocks (black) and low liquidity stocks (grey). Information on *AOU*5 and *AOU*25 in Appendix C reveals similar features. Graph 1 illustrates the expected spray shape predicted by the shock response function of ACD models studied by Fernandes and Grammig (2006).[15] In a balanced and efficient market, mispricing of fundamentals should be symmetric around zero, meaning overreaction should counterbalance underreaction. Therefore, we should expect top-down symmetry across the *y*-axis at zero. Additionally, there should be symmetry between positive and negative *SAC* values of equal magnitude (left-right symmetry across the *x*-axis at zero, indicated by a solid black vertical line), as well as symmetry between high and low liquidity stocks. Graph 1, however, reveals noticeable left-right asymmetry and differences between low and high liquidity stocks. The left-right asymmetry suggests that subsequent prices overreact and underreact differently in faster-than-expected markets (positive *SAC*) compared to slower-than-expected markets (negative *SAC*). Additionally, low liquidity stocks appear to overreact and underreact more than high liquidity stocks, especially with larger *SAC*.

We test whether this is the case by regressing *AOU*15 on *SAC* and a liquidity dummy:[16]

$$\frac{1{,}000}{15} \times \sum_{n=1}^{15} \Delta\varphi_{i+n} q_{i+n} = c_{m,r} + (\gamma_{m,r} + \delta_{m,r} * L_i) * SAC_i + u_i, \quad (10)$$

[14] We also test for asymmetry across buys and sells but find none (see online Appendix C).
[15] Moderated, or flipped, by whether q_{i-1} is +1(buy) or -1(sell), as in Equation (7).
[16] While the exact relationship is polynomial, a simple test of linear slopes should suffice.

where the dependent variable $AOU15_i \equiv (1/15)\sum_{n=1}^{15} \Delta\varphi_{i+n} q_{i+n}$ is scaled up by 1000; $(c, \gamma, \delta)' \equiv \boldsymbol{\beta}$ is a vector of coefficients; $m = \{SAC_i < 0, SAC_i > 0\}$; and $r = \{AOU15_i < 0, AOU15_i > 0\}$, and L=1 for High Liquidity stocks, and zero otherwise. This empirical specification captures the impact of shocks in arbitrage capacity, SAC_i, (i.e., higher or lower than anticipated activity from a specific agent type), on *subsequent* price deviations from fundamentals. Consequently, it serves as an empirical impulse response function of prices to innovations in trading intensity or arbitrage capacity. According to the impulse response function of ACD models (see Fernandes and Grammig, 2006), innovations in trading intensity should symmetrically affect expectations of subsequent trading intensity in a recursive manner. These recursive expectations, Θ_i, should be reflected in the information and liquidity price components, θ_i and φ_ι, of subsequent price changes and, consequently, symmetrically on the SAC_i. Any asymmetry would imply systematic price deviations from fundamentals that are *disproportionate reactions to surprises* in arbitrage capacity as applied to trades. A positive (negative) trading intensity shock would imply a faster (slower) than expected market and more (less) capital than anticipated pursuing an arbitrage opportunity. A higher γ coefficient for faster market conditions would indicate that higher-than-anticipated arbitrage capacity has a more intense impact on subsequent mispricing. Given that this would be due to a larger *surprise* in trading intensity (realised) rather than higher *expected* trading intensity (modelled), the price impact would be consistent with the crowdedness effect. Similarly, the δ coefficient captures systematic incremental differences in the impulse response function of heavily traded stocks compared to other stocks.

We run this regression once, using identity dummies to separate combinations of *m* and *r*. These combinations correspond to the following quadrants of Graph 1: Quadrant 1, where both AOU_i and SAC_i are positive; Quadrant 2, where AOU_i is positive and SAC_i is negative; Quadrant 3, where both are negative; and Quadrant 4, where AOU_i is negative and SAC_i is positive. These quadrants are abbreviated as Q1 (top right), Q2 (top left), Q3 (bottom left), and Q4 (bottom right).

The slope estimates in each quadrant are presented in the first column, entitled "All", of the top three panels of Table 2.[17] Rows entitled "Low Liquidity" present estimates of γ, and rows entitled "High Liquidity" present estimates of δ, which is the incremental contribution of High Liquidity stocks to γ. The parentheses contain *t*-statistics. The tabulated slope estimates are significant in all quadrants and have the expected sign, indicating a significant relationship between mispricing and unanticipated arbitrage capacity throughout, as expected. The R^2 values imply that, on average and in a linear form over all transactions, variations in unanticipated arbitrage capacity explain around 31% of variations in subsequent mispricing, or 38% when the liquidity dummy is activated. This is substantial explanatory power.

Contrary to expectations of a balanced market, however, significant asymmetries exist in this relationship. The slope estimates for "All" transactions are greater in Q4 than Q1 and in Q3 than Q2. This indicates top-down asymmetry, and that overreaction is not counterbalanced by underreaction. The slope estimates are also greater for Q1 than Q2 and for Q4 than Q3, indicating left-right asymmetry and that the market overreacts and underreacts more in faster-than-expected markets (positive *SAC*) compared to slower-than-expected markets (negative *SAC*). Additionally, the slope estimates for low liquidity stocks are higher than those for high liquidity stocks. The statistical significance of almost all of these differences is confirmed by the Wald tests reported in the first column of each of the bottom three panels of Table 2 (*p*-values in parenthesis), where "Q1 vs Q2" and "Q4 vs Q3" test left-right asymmetries, while "Q4 vs Q3" and "Q2 vs Q3" test top-down asymmetries.[18] These reveal significant asymmetries between slower-than-anticipated market conditions and faster-than-anticipated

[17] From space constraints, we report *t*-tests and *p*-values but not the asterisk notation of significance (***, **, *).
[18] The exceptional insignificance of the test on "Q1 vs Q4" and "Q2 vs Q3" for High Liquidity stocks indicates no top-down asymmetry for these stocks. "Q2 vs Q3" is insignificant for "All" stocks but significant for low liquidity stocks. The coefficient comparison for High Liquidity stocks is conducted on $\gamma + \delta$ and not solely on δ.

market conditions, high and low liquidity stocks, and overreaction and underreaction (with the last being slightly weaker in high liquidity stocks). Further, values in the "News" columns in Table 2 show that these asymmetries largely persist across days of good, bad, and no news, albeit with some exceptions.[19] Interestingly, High Liquidity stocks exhibit left-right asymmetry only, and consistently across days, indicating distinctly different mispricing in faster-than-expected markets compared to slower-than-expected markets. Notably, contrary to the concept of "congestion," which theoretically should only appear in fast markets, the Wald test values for left-right asymmetry are *negative* on good-news days across stocks of all liquidity levels, suggesting that mispricing is more pronounced when market activity is *slower* than expected. Furthermore, on no-news days, overreaction is not counterbalanced by underreaction for low-liquidity stocks. These asymmetries align more with the presence of crowdedness than with congestion, which results from mere liquidity squeezes.

4.2. Asymmetries in mispricing uncertainty (risk) and the resolution of crowdedness

In terms of mispricing risk, Graph 1 shows a greater *dispersion* of mispricing for positive *SAC* than for negative *SAC*. We test this asymmetry by an *F*-test on the ratio of the variances of *AOU*, $\sigma^2_{AOU15,Positive\ SAC}/\sigma^2_{AOU15,Negative\ SAC}$.[20] The results, reported in the first column entitled "All" in Panel A of Table 3 (*p*-values in parenthesis), are almost all significantly higher than one. Therefore, traders overreact and underreact with greater uncertainty when higher-than-anticipated arbitrage capacity is applied compared to when lower-than-anticipated arbitrage capacity of equal magnitude is applied. Moreover, this asymmetry is not indicative of a balanced market.

[19] The exceptions are: "Q1 vs Q4" during bad news days and "Q2 vs Q3" during no news days for "All" transactions, indicating no overall top-down asymmetry; "Q2 vs Q3" during no-news days and bad-news days for Low Liquidity stocks, indicating no top-down asymmetry in slow markets; and "Q1 vs Q4" and "Q2 vs Q3" during all days for High Liquidity stocks, indicating no top-down asymmetry at all for these stocks.
[20] The findings are qualitatively similar for *AOU*5 and *AOU*25 (see online Appendix C).

The first column of Panel B of Table 3 presents a similar *F*-test but on the ratio $\sigma^2_{AOU15,Low\ Liq.}/\sigma^2_{AOU15,High\ Liq.}$, which should be equal to one if mispricing risk is symmetrical across stocks of different liquidity levels. The tabulated values are all greater than one and significant and, outside the middle range of *SAC*, increase with the magnitude of *SAC*. Thus, Low Liquidity stocks react significantly more than High Liquidity stocks to shocks in arbitrage capacity. Consequently, liquidity variation across stocks appears to be an important determinant of their ability to absorb subsequent uncertainty in mispricing that follows greater shocks in applied arbitrage capacity. This reinforces the evidence presented in Section 4.1 of a stronger crowdedness effect in less liquid stocks. Finally, Panel C of Table 3 presents *F*-test results on variance ratios across types of news and agents. Mispricing uncertainty is higher during days of bad news, and for algorithmic trades than institutional and retail trades.

In summary, there are significant asymmetries in the dispersion of the market's reaction to unanticipated arbitrage capacity. On average, the market reacts with greater uncertainty in faster-than-expected conditions, for lower liquidity stocks, during days of bad news than during other days, and for algorithmic trades than institutional and retail trades. High liquidity stocks are better at absorbing liquidity-driven shocks that arise from crowdedness, most likely due to greater depth. This aligns with our zero-profit condition modelling, as all relevant costs are more readily and swiftly recovered in more liquid environments, reducing pricing sensitivity to unanticipated arbitrage capacity. In such environments, the market requires more significant liquidity shocks to exhibit similar overreactions or underreactions.[21]

[21] While uncertainty in overreaction and underreaction is one of the symptoms mentioned by Stein (2009) of crowdedness emanating from unanticipated arbitrage capacity, in our UHF setup it is a natural consequence of the equilibrium mechanism that incorporates the ACD shock response function. Asymmetries in this uncertainty, however, are not, and the evidence we report points towards a number of possible issues. The first is indeed the presence of crowdedness. However, other reasons are also possible. For example, the possible existence of omitted variables that may increase the signal-to-noise ratio of order flow and applied arbitrage capacity beyond our pricing model, or other behavioural effects, cannot be entirely ruled out, albeit the crowdedness interpretation is more likely given the enhanced features of our pricing model. This inference is supported by our prediction analyses in Sections 4.3 and 4.4.

It is interesting to measure the length of time over which these asymmetries in mispricing risk persist. Graph 2 in Table 1 plots the standard deviation of *AOU* over ‘bins’ of the next 5, 15, 25, 50, 75, 100, 125, 200, 250, and 500 transactions. The grey line shows that this standard deviation declines with the number of future transactions, indicating a dissipation of mispricing risk and a resolution of uncertainty in mispricing over longer horizons. Tabulated below the graph are values of an *F*-test (and its *p*-values) on the *incremental decrease* in the variance of *AOU* from one bin to the next from left to right, and the average and the median time it takes for these transactions to occur. The *F*-test shows that the incremental dissipation is significant until transaction 150 and, consequently, most uncertainty in mispricing is resolved by the time 150 transactions have occurred (or 100 transactions if 5% is taken instead of 10% as the cut-off significance level). This takes an average time of 1.73 min or a median time of 0.23 min (100 transactions take an average of 1.15 min or a median of 0.15 min). Although short, this timescale is relatively very long for algorithmic trading. We consider this an early indication that mispricing uncertainty due to crowdedness, which is a liquidity effect emanating from surprises in arbitrage capacity, persists beyond algorithmic timescales. Next, we explore this further within the context of UHF phenomena, algorithmic trading, and institutional trading.

4.3. Does crowdedness predict ultra-high frequency extreme events?

Important to regulators, market operators, and investors are the possible causes of the frequent sudden failure of markets, such as flash crashes and price dips, or their flip counterparts, price bubbles and spikes. Could crowdedness due to uncertainty in arbitrage capacity, or irrational behaviour by agents, predict UHF phenomena? Although causation is difficult to isolate at high frequency, we draw meaningful inferences through a variety of methods. We conduct two analyses. The first tests predictability on a trade-by-trade basis, and the second uses interval measures to allow comparison with the VPIN of Easley et al. (2011a).

4.3.1. Trade-by-trade predictability

We start by formulating two new UHF measures of crowdedness: $Crowd_i = |OU_i|/SAC_{i-1}$ and $|Crowd_i| = |OU_i|/|SAC_{i-1}|$, where $OU_i = \Delta(\phi_i q_i)$ is the overreaction and underreaction in trade *i*. Both measures capture the mispricing of a trade per unit *SAC* of the *previous* trade, but the first measure is signed and distinguishes faster-than-anticipated market conditions (when *Crowd*>0) from slower-than-anticipated market conditions (when *Crowd*<0). Next, we investigate how these measures predict UHF extreme events (crashes and spikes), buy and sell runs (herding), heightened demand for immediacy (impatience), increases in trading costs, and the intensity of presence of algorithmic, institutional, and retail trades. To this end, we follow the previous literature (e.g., Johnson et al., 2013) in defining the following variables:

1. *UHF.* A dummy variable that counts ultra-high-frequency extreme price events on one side of the order book that feature price crashes or spikes:

   $$UHF = \begin{cases} 1, & if\ duration < 1{,}500ms\ and\ min_{sidedness} = 10\ and\ min_{|\Delta P|} = 0.8\% \\ 0, & elsewhere \end{cases},$$

   where, *ms* = milliseconds, and *sidedness* = |trade imbalance|/number of observations = $|\#_{buys} - \#_{sells}|/\#_{trades}$ is a modified version of Sarkar and Schwartz' (2009) measure based on correlations that captures asymmetric-information-motivated trading. Additionally, see Johnson et al. (2013) for robustness on the 1,500*ms* length.

2. *Runs.* This variable is used in the overreaction literature and captures the average intensity of directional trading over several trades (e.g., herding):

   $$Runs = \left(run_{buys} + run_{sells}\right)/\#_{trades}, \text{ where}$$

   $$run_{buys} = \begin{cases} Number\ of\ buys, & if \geq 2 \\ 0, & elsewhere \end{cases}.$$

   This measure has a maximum of 1 when all trades are in one run. Higher values indicate more trades occurring in a specific direction and lower values indicate more random trading.

3. *Algorithmic (Algo.)*. A dummy variable that counts trades proceeding faster than the reactive ability of humans (i.e., machine trades; see Johnson et al., 2013):

$$Algo. = \begin{cases} 1, & if\ duration < 650ms \\ 0, & elsewhere \end{cases}$$

   We also distinguish trades with duration < 1ms (called *Algo2*) that may be involved in snipping or ‘arms races’ (see Haldane, 2011; Budish et al., 2015; Aquilina et al., 2022).

4. *Institutional (Inst.)*. A dummy variable that counts large-value trades as a proxy for the presence of institutional trading (see e.g., FINRA rule 5320; Mackintosh, 2020)[22]:

$$Inst. = \begin{cases} 1, & if\ trade\ value > \$100k \\ 0, & elsewhere \end{cases}$$

   All other trades are classified as ‘*Retail*’ trades.

5. *Trade-to-order ratio (TR)*. This is the ratio of the volume of trades to the volume of best quote revisions. It captures the presence of market orders relative to limit orders and proxies the relative demand for immediacy (liquidity) over price, or the degree of “impatience.”

6. *Spread*. This is the bid-ask spread in $ just before a trade. It reflects posted trading costs.

Basic statistics of the first 4 variables are reported in Panel A of Table 1 and, in more detail, in Table A.1 in the online Appendix A. Out of the 230,084,293 trades in the sample, 73.12% are algorithmic, of which 9.69% are of sub 1ms duration, 3.3% are institutional, and 23.58% are retail. There were 1472 UHF extreme events during the sample period, occurring most frequently in the Apple Inc stock (281) followed by the Microsoft stock (137), and least frequently in the TRV stock (3) followed by the AXP stock (4). Every other stock experienced at least 11 such events during the sample period.

We first confirm the presence of crowdedness in these trades. The last three columns of Table 2 show that the asymmetries in all trades described in Sections 4.1 and 4.2 largely exist

[22] The Financial Industry Regulatory Authority (FINRA) rule 5320 that prohibits trading ahead of customer orders (front running) refers to institutional accounts (Rule 4512(c)), orders of 10,000 shares, and orders with a minimum value of $100k, as “large orders”. We also consider alternative definitions of large and sub-penny trades for robustness. The results, in Tables C.10 and C.11(A, B) of online Appendix C, corroborate those reported here.

also in algorithmic, institutional, and retail trades when considered separately, especially left-right asymmetry between faster- and slower-than-expected markets (Q1 vs Q2 and Q4 vs Q3). There are some exceptions. Retail trades in high-liquidity stocks do not exhibit significant top-down asymmetry (Q1 vs Q4 and Q2 vs Q3), and those in low liquidity stocks exhibit top-down asymmetry in slow markets (Q2 vs Q3) but not in fast markets. Both algorithmic and institutional trades exhibit significant left-right and top-down asymmetries in mispricing, regardless of stock liquidity. The last 6 columns of Panel A of Table 3 show that, in general, algorithmic and retail trades also exhibit strong asymmetries in the *uncertainty* of mispricing regardless of the level of stock liquidity, while institutional trades show much weaker asymmetry and only in a few bins of *SAC*. Panel B of Table 3 shows that asymmetries in mispricing uncertainty are much greater in low-liquidity than in high-liquidity stocks. Panel C shows that, in most SAC bins, they are greater in algorithmic trades than in retail trades, and in retail trades than in institutional trades. These results confirm the presence of the crowdedness effect in algorithmic, institutional, and retail trades, albeit to varying extents.

To investigate the predictive power of crowdedness, we run the following regressions:

$$Q_{i+s} = c + a(|Crowd| \text{ or } Crowd) + CV_i + u_i + e_i \tag{11}$$

where Q_{i+s}= (*UHF, Algo., Runs, Inst., TR, Spread*)' is a vector of dependent variables indexed by *s* = 5, 25, 50, 100, and 150 bins of *prospective* transactions over which these variables are measured; CV_i = *(duration, trade volume, order count, sum of volume at BBO)*' is a set of control variables measured at the time of trade *i*; *c* and *a* are coefficients; u_i are fixed effects; and e_i are errors. All variables are proportions of the number of trades in the prospective transaction bins, except the *Spread*, which is an average in each bin.

The estimation results are presented in Table 4 where the explanatory variable *Crowd* is split into positive and negative parts (*Crowd*+ and *Crowd*-) to reveal differential effects between faster and slower markets. The most prominent result is that |*Crowd*| is significantly positively associated with the *prospective* values of all six dependent variables for up to 150 transactions ahead (intensity of runs to 50 transactions ahead and trade/order ratio to 100 transactions ahead). The R^2 values range from 5.25% to 38.12% and are higher for shorter bins where they range from 11.94% to 38.12% over the next 5 transactions. This is sizeable explanatory power. Thus, crowdedness is a strong predictor of UHF extreme events, the proportions of algorithmic and institutional trades, the intensity of runs, the demand for immediacy, and trading costs. Further, the magnitude and significance of the slopes generally decline over longer bins, indicating lower predictive power over longer horizons. The exception is the spread, where the slope magnitude increases monotonically, indicating higher predictive accuracy for trading costs over longer horizons. This increasing sensitivity of trading costs to crowdedness coupled with a declining sensitivity of the trade/order ratio over longer horizons indicates that although the impatience for liquidity becomes less sensitive to mispricing per unit shock in arbitrage capacity, the effect on trading costs apparently persists. This may make certain participants, such as institutions, more cautious in entering a crowded market because trading costs become more sensitive to liquidity variations, increasing their future uncertainty. We investigate this further in our interval analysis in Section 4.3.2.

Regarding the results on *Crowd+* and *Crowd-* in Table 4, their slopes are all significant, but those of *Crowd+* are smaller in magnitude than those of *Crowd-* except for algorithmic trading during the next 5, 25, and 50 trades, and the intensity of runs over the next 5 trades. This indicates that the prospective presence of algos over the next 50 transactions, and of runs over the next 5 transactions, is more sensitive to crowdedness in faster- than in slower-than-anticipated markets. Rows entitled $t_{(+)\text{-}|\text{-}|}$ present *t*-tests (*p*-values in parenthesis) of the difference in slopes between *Crowd+* and *Crowd-*. These show that asymmetry in the sensitivity to crowdedness between faster and slower markets persists mainly over the next 5 transactions for all variables except *UHF*. Note that $t_{(+)\text{-}|\text{-}|}$ for the next 5 transactions is significant and *negative* for institutional trades, trade-to-order ratio, and the bid-ask spread, indicating a higher probability of increases in these variables during *slower*-than-anticipated markets. Conversely, $t_{(+)\text{-}|\text{-}|}$ for the next 5 transactions is significant and *positive* for algorithmic trades and the intensity of runs, indicating a higher probability of increases in these variables during *faster*-than-anticipated markets. This asymmetry does not exist for UHF events, even though, like the other variables, *UHF* is significantly predicted by crowdedness over horizons to 150 transactions. Finally, a *threshold* value of crowdedness, beyond which mispricing increases substantially but at a decreasing rate, is estimated at around 5 cents.

In summary, crowdedness at trade level is a strong predictor of UHF extreme events, algorithmic trades, herding, institutional trades, impatience for liquidity, and spreads over the next 150 transactions. It also helps differentiate patterns across fast and slow market conditions over the short time scale of the next 5 transactions, which have an average duration of 3.6 sec.

4.3.2 Interval predictability of crowdedness on UHF events and a comparison with VPIN

We now investigate the predictive power of crowdedness on UHF events in interval measures and compare it to the Volume Synchronised Probability of Informed trading (VPIN) of Easley et al. (2011a). Additionally, we analyse the likely causes of UHF extreme price events. The primary relevance of VPIN to our study is that it is designed to capture costs related to order flow toxicity, linked by some scholars to short-term price deviations and corrections arising from disruptions in order flow. Generally, VPIN is the ratio of average order imbalances over a sample length defined by volume "buckets." The numerator of this ratio proxies for expected directional or informed trading, and the denominator proxies for the total number of trades over which this occurs. Several studies, such as Abad and Yagüe (2012) and Andersen and Bondarenko (2014a, b), argue that the absolute magnitude of VPIN is highly sensitive to the selection of the volume bucket size and the sample length. We address these concerns in our calculation of VPIN, which we fully describe in the online Appendix D. It is interesting to investigate the incremental predictive contribution of our *Crowd* measure on UHF events relative to that of VPIN, algorithmic trading, institutional trading, and their interactions.

We begin by estimating the following regressions in the levels and the lags using interval measures, as VPIN is an interval measure:

$UHF_t = c + aVPIN_t + \beta \sum_{trades_t} |Crowd| + \gamma Algo._t + \delta Inst._t + \boldsymbol{\delta index}_t + \boldsymbol{\zeta} CV_t + u_t + e_t,$

$UHF_t = c + aVPIN_{t-1} + \beta \sum_{trades_{t-1}} |Crowd| + \gamma Algo._{t-1} + \delta Inst._{t-1} + \boldsymbol{\delta index}_{t-1} + \boldsymbol{\zeta} CV_{t-1} + u_t + e_t,$ (12a and 12b)

where t indexes the $interval = (5'', 30'', 60'', 5', 30', 60')'$ over which all variables are calculated; ($''$) denotes seconds and ($'$) denotes minutes; *UHF*, *Algo.*, and *Inst.* are redefined as the numbers of trades classified as UHF events, algorithmic, or institutional per stock per interval; $\boldsymbol{index}_t = (Algo._t \times \sum_{trades_t}|Crowd|, VPIN_t \times \sum_{trades_t}|Crowd|)'$ is a vector of two interaction terms of |*Crowd*| with *Algo.* or *VPIN*; *CV* = (*conditional variance of* Δp_t (*C. Var.*), *average spread*, *average trade/order ratio*, *average duration*, *average volume*)$'$ is a set of control variables calculated over interval *t*; u_t are fixed effects; and e_t are errors. We include *C. Var.* in *CV* to account for evidence in the literature that volatility is a predictor of turmoil.

The estimation results are presented in the first column of each interval panel in Table 5.[23] First, R^2 of the level regressions range from 37.47% to 57.16%, indicating that a substantial proportion of variation in UHF extreme events is predicted by the variables. Second, the most notable result from Table 5 is that both the level and the lag of |*Crowd*| are positive and significant, even with the inclusion of other variables. Thus, |*Crowd*| captures significant incremental information. Third, the coefficient of |*Crowd*| is more significant than that of *VPIN* for level intervals of 30$''$ or longer, and more significant than those of *Algo.* and *Inst.* for all intervals. This indicates that crowdedness is a more important predictor of UHF events over these horizons than VPIN or algorithmic and institutional trading. Further, the significance of

[23] Inferences focus on the degree of significance of the coefficients since the variables are not normalised for the coefficient magnitudes to be comparable. For brevity, estimates of *CV* coefficients other than *C. Var.* are not reported. All results are available from the authors. We use *italics* for variables we calculate.

VPIN drops considerably to marginal or insignificant levels at intervals of 30″ or longer in the levels and at intervals longer than 60″ in the lags. The drop in *VPIN*'s significance is even larger when its interaction with |*Crowd*| is activated (Table 5) than when it is muted (Table C.12 in the online Appendix C).[24] When this interaction term is activated, *VPIN* loses significance for level intervals longer than 30″, while |*Crowd*| remains significant throughout. Furthermore, *VPIN*'s coefficients turn negative in lagged regressions at intervals 30′ and 60′.

Similar, but stronger, results are observed for *Algo*. Specifically, its significance diminishes substantially, and its coefficient becomes negative for most intervals of 30″ or longer when its interaction with |*Crowd*| is considered (compare Tables 5 and C.12). Consequently, crowdedness is a stronger predictor of UHF events than algorithmic trading, carrying information that at least partially subsumes that in *Algo. Inst.*, by contrast, remains insignificant throughout. This clearly indicates that trade size alone does not predict UHF events and is only useful when combined with volume and speed, being trade dimensions integral to algorithmic trading and the calculations of |*Crowd*| and *VPIN* (albeit in a more aggregated form than in |*Crowd*|). Therefore, it appears that, on average, large trades alone do not trigger UHF extreme events. Instead, crowdedness is a more significant, stable, and reliable predictor of these events compared to VPIN or algorithmic trading. The predictive power of *VPIN* and *Algo.* is notably influenced by crowdedness and is almost subsumed by it.

Collectively, these results may suggest that |*Crowd*|, *VPIN*, and *Algo.* are correlated. While such correlation might be anticipated in interval measures influenced by trading volume and speed, it raises concerns about potential multicollinearity and obscures issues of causation. To address these concerns, we first assess the extent and nature of multicollinearity by reporting the Variance Inflation Factor (VIF) in Table 5.[25] The lowest VIF value of 1 is observed for the

[24] Table C.12 presents estimation results over more intervals and when ***index***, *Algo.*, or *Inst.* are excluded.
[25] These are reported as the second number within the parentheses that appear below the coefficient estimates. A VIF=1 indicates no multicollinearity, while values above 1 indicate higher levels of multicollinearity.

conditional variance of price change (with the exception of a value of 2 in the lagged 30″ interval), indicating almost no multicollinearity overall for this variable. The next lowest VIF value, ranging from 1.2 to 2.2, is reported for |*Crowd*|, indicating a small level of multicollinearity that reflects the correlations mentioned above. All other variables, including the interaction terms, exhibit higher levels of multicollinearity. Notably, *VPIN* shows the highest VIF values in all regressions except one (60″ interval), with values ranging from 1.4 to 9.7, clearly indicating substantial multicollinearity relative to the other variables. Thus, while information overlap exists, its extent varies across variables and may obscure inferences about which variable *causes* UHF events or acts as a *trigger* to the other variables.

We address this causation through several approaches that further analyse the multicollinearity indicated by the VIF values. First, the previous inclusion of interaction terms in the interval regressions shows that |*Crowd*| has a *direct* predictive power on UHF events, even in the presence of other variables. Further, by omitting the interaction terms and comparing the results (Table C.12), we capture the *moderation* effect of variables on each other. In this context, |*Crowd*| remains significant with interactions present, while *VPIN* and *Algo.* decrease in significance, change coefficient signs, and exhibit higher VIF values. This indicates that |*Crowd*| moderates the impact of *VPIN* and *Algo*. in predicting UHF events, rather than the reverse. Third, we explore the potential *indirect mediation* effect of |*Crowd*| on *UHF* through *VPIN* and *Algo*. This is reported as *Ind.* in Table 5, along with its (2.5%, 97.5%) bootstrapped confidence interval, enclosed in parentheses in adjacent columns.[26] All confidence intervals do not bracket zero, and their mid values are close to those of *Ind.*, supporting a significant mediation effect of |*Crowd*| on *UHF* through *VPIN* and *Algo.* combined, which explains the correlations reported above. We further use Sobel's (1982)

[26] The indirect effect of |*Crowd*| on *UHF* through *VPIN* and *Algo* is the change in *UHF* for every unit change in |*Crowd*| that is mediated by *VPIN* or *Algo*. *Ind.* is Judd and Kenny's (1981) measure of the difference between the partial and simple coefficients on |*Crowd*| from a regression of *UHF* on |*Crowd*| and *VPIN* or *Algo.* and from another regression of *UHF* on |*Crowd*| only. Sobel's (1982) method used below is based on the delta method.

method to decompose this combined mediation effect into components attributable to *VPIN* and *Algo.*, reported separately as *V* and *A* in the row labelled *V* | *A* in Table 5. The associated confidence intervals confirm a significant indirect mediation effect through each variable, with *V* values exceeding *A* values, indicating greater mediation through *VPIN* than through *Algo.* This suggests that *VPIN* carries information on crowdedness but also incorporates other information, as it is based on total price impact rather than solely on liquidity costs. Thus, crowdedness is a stronger and purer direct and indirect predictor of UHF events than *VPIN* or *Algo*., permeating both variables, particularly *VPIN*. Fourth, to eliminate multicollinearity and clarify causation, we estimate LASSO regressions to reduce dimensionality through variable selection.[27] The results (Table 5) provide strong evidence that |*Crowd*| remains a significant variable in all estimations and, in some estimations, is the only variable that persists. In contrast, *VPIN* is eliminated in all LASSO regressions of intervals of 60′′ or longer in the levels and in all lagged regressions. When *VPIN* appears significant, its significance is much weaker than that of |*Crowd*|. *Algo.* and *Inst.* are eliminated in all LASSO regressions, clearly indicating that they are entirely subsumed by crowdedness. The interaction terms are significant only in intervals of 5′ or less in level regressions and are eliminated in all lagged regressions. Accordingly, *VPIN* and *Algo*. have an *indirect* impact in some intervals only, *driven* mainly by crowdedness. Thus, when *VPIN* and *Algo.* contribute in predicting UHF events, it is likely due to crowdedness.[28] Furthermore, the reduction in R^2 between non-LASSO and LASSO regressions confirms that |*Crowd*| explains the largest proportion of *UHF* variations. These results provide clear evidence that crowdedness is a much stronger predictor of UHF extreme

[27] These Least Absolute Shrinkage and Selection Operator regressions optimise a trade-off between model sparsity and prediction accuracy by penalising coefficients of variables that do not contribute sufficiently to predictive power, such as those that are highly collinear. We estimate these regressions using the Bayes Information Criteria to optimise the shrinkage parameter for variable selection, and 70% of the sample for training.
[28] We also analyse lead-lag relationships and Sims causality through VARs on the interval variables. The results, reported in Appendix C, show that crowdedness *causes* the other variables and is a catalyst and a *trigger* of algorithmic trades when they play a role in UHF events by contributing to liquidity spirals and order flow toxicity.

events than VPIN or algorithmic and institutional trading. It carries incrementally different information and acts as a trigger to algorithmic trading during liquidity spirals.

The conditional variance of price change is the only variable, aside from crowdedness, that shows significant direct predictive power on UHF events, underscoring the high level of volatility associated with these events. However, the significance of this variable diminishes considerably over longer intervals and vanishes in lagged regressions of 30′ or longer and in LASSO regressions of 5′ or longer. In contrast, |*Crowd*| remains significant in all LASSO regressions, both level and lagged. This is a strong result, as volatility is regarded as a primary predictor of UHF events. Our results indicate that, while the predictive power of volatility remains significant, it is not as persistent as that of crowdedness over longer intervals.[29]

Another noteworthy observation is that all coefficients on the level and lag of *Inst.* are negative and mostly insignificant, particularly when the interaction terms are included. The negative coefficients, where significant, suggest the withdrawal of institutions (large trades) just before and during UHF events, potentially reducing market liquidity and increasing the proportional presence of small and opportunistic players. This could further contribute to the liquidity spirals often cited as the cause of flash events – an inference consistent with discussions in the literature, such as the joint reinforcement of market liquidity and funding liquidity and the flight to quality mentioned by Brunnermeier and Pedersen (2009).

Figure 1 plots 9 measures during the 6 May 2010 flash crash, which occurred from 14:32hr to 15:08hr.[30] Volatility spiked at 11:35hr, then fluctuated wildly around a mild uptrend until 14:05hr. Apart from a small rise at 14:34hr, it continued to decline during the crash, with a sudden drop at 15:05hr. The correlations between *VPIN*, *Algo*. and |*Crowd*| are evident in a

[29] Considering variance as a control variable partially accounts in our sample for Abad et al.'s (2018) critique that ex ante realised volatility subsumes VPIN's identification of the price impact due to toxicity.
[30] The CFTC concluded 5 years later that "spoofing" by a single trader in E-mini S&P futures significantly contributed to the conditions that led to the crash. Figure 1 shows that crowdedness in Dow stocks increased during the period (11:17–13:40hrs) in which the trader used his 'dynamic layering' programme on E-minis.

common rising trend before the crash, which persisted for an additional 7 minutes. However, |*Crowd*| exhibited a stronger and clearer rising trend above its threshold value of 5 cents, beginning earlier at around 12:34hr. Its sudden drop at 14:45hr coincided precisely with a spike in the *Spread*, which disrupted the liquidity spiral by reducing the opportunity of latency arbitrage, thereby helping to mitigate the crash. |*Crowd*| then decreased but remained above its threshold for the remainder of the day. Institutional trading was noticeably lower during the crash period. These observations align with our findings across all 1472 UHF events analysed.

The above results prompt the question: what does |*Crowd*| capture that VPIN and price volatility do not, or not as precisely? |*Crowd*| has several distinct features. First, it is based on a pricing model of trades, whereas VPIN is not and instead considers order imbalances rather than trades. Second, our mispricing measure focuses on the liquidity cost component of price changes after filtering out asymmetric information effects and their dynamic interactions with expected liquidity (reflexivity). |*Crowd*| captures the rate of the market's overreaction in unexpected liquidity costs per unit of uncertainty in arbitrage capacity, providing a "purer" measure of the costs most relevant to order flow toxicity. Third, our modelling of arbitrage capacity is more precise and innovative. It differentiates expected from unexpected capacity and estimates these from trades rather than orders, thereby aligning estimates with the realised capacity actually applied by traders to arbitrage opportunities. Additionally, expected capacity is estimated for three distinct agent types while accounting for the amount, speed, and intensity of their presence, allowing for a more nuanced consideration of agent specific reactions and interactions. Consequently, |*Crowd*| captures market overreactions to surprises in agents' arbitrage capacity. In contrast, VPIN relies on order imbalances that reflect 'intended' rather than 'applied' trading actions, and uses *total* price reaction (numerator) and, rather controversially, specified volume buckets (denominator) to estimate the level of trading intensity. Total price reaction, however, conflates interacting and *opposing* asymmetric information and liquidity effects, which may offset each other in certain market conditions (see

Ibrahim and Kalaitzoglou, 2016). Thus, VPIN may not relate as clearly to toxicity or other liquidity-related UHF phenomena. |*Crowd*| focuses on the liquidity-related mispricing implications (numerator) of innovations in the amount, speed, and presence of agents' liquidity (denominator), offering a finer breakdown of price reactions and a greater focus on liquidity. Unlike VPIN, |*Crowd*| does not focus on trading intensity, but accounts for its *expected* role in both the liquidity and information components of price and filters out the latter. It captures surprises in liquidity-related effects while accounting for the expected presence and trading intensity of agents. This provides a more precise link to temporary liquidity-related phenomena since surprises in capacity elicit diverse reactions across agents unrelated to fundamentals, especially at high frequency with machine agents acting at speed and when liquidity fears override information concerns. Our measure, therefore, better relates to toxicity, liquidity spirals, and UHF phenomena, and our empirical evidence supports this inference.

5. Some implications and recommendations

There are several implications for our results. We present here a selection and report more detail in the online Appendix E. First, a general and direct primary use of our crowdedness measure is in predicting flash crashes, spikes, and the other UHF phenomena analysed in Section 4. Second, crowdedness imposes significant economic costs on investors and market makers. Table C.15 presents estimates of these costs for hypothetical "surprise" trades. For an average-sized trade executed 10 times faster (i.e., a typical algorithmic trade), crowdedness cost can reach \$41.37, or 2.01% (0.20%) of trade value for \$10 (\$100) stocks. For an extreme trade that is 50 times larger and faster than average, the cost can rise to \$2,272, or 2.21% (0.22%) of trade value for \$10 (\$100) stocks. Accordingly, a trading strategy to mitigate crowdedness costs over the next 150 transactions can be proposed. Investors should execute multiple small orders to buy low-crowded, high-denomination, high-liquidity stocks, and a few large orders to sell highly crowded, low-denomination, low-liquidity stocks. This option-like strategy capitalizes on the “crowdedness premium” across stocks and order sizes, particularly when crowdedness is high. Its hedge ratio of low-to-high crowded stocks could be adjusted based on changing levels of market crowdedness and trading intensity. Investors can also use options on these stocks, if available, to construct strategies to hedge the *delta*, *gamma, vega/kappa*, or *theta* of mispricing risk emanating from unanticipated capacity. If short selling and liquidity restrictions bind, temporarily halting trading might be advisable until crowdedness costs decrease. This effectively serves as a self-imposed “circuit breaker”.

Estimates of crowdedness costs are also relevant to market makers. Huang and Wang (2009), for instance, show that even small costs for maintaining market presence prompt market makers to limit risk exposures, failing to offset liquidity imbalances unless substantial price adjustments are made to compensate for the additional risky inventory. Therefore, estimates of crowdedness costs can assist market makers in better managing their inventories and setting appropriate spreads during liquidity imbalances. Incorporating predicted crowdedness costs in the spread would compensate market makers for liquidity and penalise prospective trades with the mispricing they cause when contributing to liquidity spirals. Wider spreads would mitigate speculative arbitrage without halting trading, functioning in a similar manner to the Anti-lock Braking System (ABS) found in automobiles. Just as ABS mitigates adverse effects of sudden stops, wider spreads would prevent the negative impacts of the sudden cessation of information and liquidity resolution in prices that accompany extended trading halts.

Another implication relates to improvements in trading rules and market design. Our results indicate that institutions, whose trades are more anchored to fundamentals than those of others, withdraw from trading during crowded conditions. Their withdrawal deprives the market from their stabilizing influence, potentially exacerbating liquidity spirals. To mitigate the adverse effects on market stability and encourage institutions to return to the market, we propose two measures for regulators and market operators. First, we recommend implementing a hybrid trading mechanism that dynamically switches from continuous trading to batch trading during crowded periods. Batch trading would reduce trading panic, mitigate unfair latency advantages, and allow more time to reassess fundamentals and replenish liquidity (see Budish et al., 2015, 2023). We suggest using the estimated $0.05 threshold, beyond which crowdedness increases substantially, as a trigger for switching from continuous to batch trading in this hybrid mechanism.[31] Second, we propose enhancing the current circuit breaker tier system, which halts trading based on price volatility. Our findings show that crowdedness is a more persistent and precise predictor of UHF events than volatility. We suggest setting the duration of trading halts based on *both* the level of crowdedness and the percentage price change. For example, halt trading for 5, 10, 30, 90 mins if the percentage price change is 5–9, 10–12, 13–19, or 20+ and crowdedness increases above 5, 10, 12, or 15 cents/share during the last 10 mins of trading, respectively. The rationale for conditioning on both crowdedness and volatility is that sometimes volatility is high but crowdedness is low, suggesting efficient pricing, while in other times the opposite is true, indicating inefficient pricing. This tapered system would better reflect the degree of mispricing and the likelihood of UHF extreme phenomena.

Regarding regulation, recent enhancements like Reg NMS aim to mitigate adverse effects of order routing, payment for order flow (PFOF), short selling, and the coordinated behaviour of retail traders who deliberately create price pressure on certain stocks. Retail platforms like Robinhood (RH) generate revenue through PFOF and short selling, using social media networks like Reddit and X (Twitter) to herd retail investors towards "meme" stocks. This trading is primarily liquidity-driven, which is the focus of our crowdedness measure. Recall that our sample includes retail behaviour, with 418 (28%) of the 1,472 UHF extreme events in 2019 occurring in Apple and Microsoft, stocks regularly held by retail platform investors. Additionally, our analysis of Google attention in Table C.9 shows significant crowdedness during high attention bad news days. Thus, both our measure and results are relevant to meme

[31] Note that the 5 cents estimate of the threshold value of crowdedness seems stable across 2019 (Table 1) and the two flash crash days of 6 May 2010 (Figure 1) and 24 August 2015 (Figure C.1 in the online appendix).

stocks and social trading because |*Crowd*| captures liquidity-based mispricing associated with uncertain demand and supply from retail platforms and elsewhere, predicting herding activity, liquidity impatience and spirals, trading costs, and resultant UHF events. These phenomena are pertinent to ongoing regulatory discussions of retail trading behaviour. As such, |*Crowd*| can be used to raise *retail investor awareness of risk levels*, not just of mispricing, but also of herding, liquidity spirals, crashes, and spikes in meme or other stocks, as well as the *risk of predatory trading* by HF and algorithmic traders who have speed advantages (Brunnermeier and Pedersen, 2005). Moreover, the rate of increase of a stock's crowdedness above its long-term threshold value – regarded as its "steady state" – can indicate the stock's stability for short-term diversification or hedging during crowded periods. Used in this manner, |*Crowd*| can measure *market stability*. The literature is divided on the impact of social investors. Barber et al. (2022), for instance, find RH investors destabilizing, while Welch (2022) finds them stabilizing as they buy during price downturns without panic or margin calls, and their aggregate portfolio has good timing and alpha. To this end, |*Crowd*| can distinguish whether buying during downturns or selling during upturns results in prices that reflect fundamentals, indicating the efficiency of the pricing mechanism for individual stocks or funds. Additionally, a higher rate of occurrence of extended trends in a stock's crowdedness suggests lower *market quality* in this stock. Therefore, |*Crowd*| can serve as a *dual measure of market quality* (pricing efficiency) *and market stability* (reduced probability of extreme events and other UHF destabilizing phenomena). Further research could explore these two aspects around recent regulatory proposals, such as the Dec 2022 Reg Best Execution and Reg NMS enhancements (relating to variable tick sizes, reduction in access fee caps for protected quotations, accelerated transparency of the best priced orders), and the Feb 2023 Disclosures on Volume-based Transaction Pricing (VTP) relating to transaction fees and rebates.

In a related context, Madhavan (2012) finds that Exchange Traded Product (ETP) prices delinked from their Net Asset Values (NAVs) on 6 May 2010, indicating distorted prices of component stocks rather than ETP pricing failure. He attributes this to increased fragmentation of the US market. We also report distorted stock prices during 6 May 2010, although we show that at UHF this was driven by uncertainty in arbitrage capacity. Conceptually, uncertainty in capacity could correlate with a UHF measure of fragmentation (which we do not test). |*Crowd*|, therefore, represents a natural UHF measure of this delinking since fundamental value for a stock is akin to NAV for a fund. Accordingly, we suggest ETP market makers use |*Crowd*| to adjust the swing factor applied to the NAV to manage demand and supply on the ETP shares during crowded markets. ETP managers typically apply pre-set swing factors, but |*Crowd*| allows for more precise calculations at UHF of a *dynamic partial swing factor* that adjusts the NAV based on the degree of crowdedness in the ETP's underlying stocks. This would pass the cost of crowdedness back to traders engaged in liquidity spirals, allowing for better quotations and pricing quality, as long-term fundamental traders would be shielded, at least partially, from temporary mispricing. Moreover, since the same logic applies to individual stocks, we generically propose publishing the level of crowdedness of stocks and ETPs alongside their prices. This would offer market participants and regulators increased awareness and transparency about the extent of mispricing, leading to improved quoting, pricing, trading, monitoring, and regulatory investigations of crashes, squeezes, and extreme events in UHF trading. Disclosing the degree of crowdedness should enhance the orderliness and stability of markets by reducing the toxicity of order flow, among other benefits. This is because liquidity providers would be better informed of the likely loss they may incur at different levels of uncertainty in arbitrage capacity.

6. Summary and conclusion

This paper proposes "reflexive crowdedness" as a mechanism through which order flow becomes toxic and develops an empirical framework for examining this mechanism in high-frequency trading (HFT). Our results show that uncertainty in agents' arbitrage capacity leads to significant mispricing in HFT. This mispricing induces noise in trading signals and triggers speculative trading. Clustering in arbitrage capacity coupled with reflexive feedback loops further amplify and propagate this noise through the price components that high-speed traders rely on as trading signals. The amplified noise, facilitated by high-speed directional traders like opportunistic algos, accelerates speculative trading and pushes the market into a liquidity spiral that leads to extreme phenomena such as flash crashes and spikes.

Our results on Dow 30 stock trades show that the surprise in arbitrage capacity (*SAC*) of a trade has substantial explanatory power on subsequent mispricing (R^2 of 31% to 38%) and mispricing risk. We detect crowdedness as asymmetries in the relationship between subsequent mispricing and *SAC*. We find that the market misprices securities more significantly and with greater uncertainty under faster-than-expected conditions for lower liquidity stocks on days of bad news compared to other days, and for algorithmic trades as opposed to institutional and retail trades. During days of good news, mispricing is greater in slow markets, distinguishing crowdedness from congestion, which only occurs in fast markets. Uncertainty in mispricing due to crowdedness persists over the next 150 transactions, taking a median time of 0.23 min to resolve. Thus, the effects of crowdedness extend beyond algorithmic timescales. We estimate that crowdedness imposes substantial liquidity costs on traders amounting to as much as 2.21% of the trade value, or higher for small denominated and penny stocks.

We formulate a new measure of crowdedness at the trade level and find that it significantly predicts UHF extreme price events, price runs, demand for immediacy, bid-ask spreads, and algorithmic and institutional trading over the next 150 transactions. Further analysis reveals that an interval-based version of this measure is a stronger and more reliable predictor of flash crashes and spikes than VPIN and price volatility. While it interacts with VPIN and algorithmic trading, our results indicate that crowdedness is the primary driver and a trigger for speculative algorithmic trading during extreme events. Additionally, our findings show that institutional investors withdraw from crowded markets due to anticipated increases in the sensitivity of trading costs to crowdedness, further contributing to market instability during extreme events.

The general implication of our results is that market instability at UHFs is not solely influenced by the presence, speed, or capital of agents but rather by the rate at which the market misprices fundamentals in liquidity costs for every unit surprise in the arbitrage capacity of agents. We recommend publishing crowdedness metrices alongside prices to inform traders of the liquidity costs they would likely incur at different levels of uncertainty in arbitrage capacity. Investors can capitalise on the crowdedness premium through targeted strategies, while market makers should reflect crowdedness costs in the spread. Exchange Traded Product managers can design partial swing factors based on crowdedness, and market operators can implement a hybrid trading mechanism that switches from continuous to batch trading along with a circuit breaker tier system based on crowdedness and price volatility. We propose our measure of crowdedness as a UHF indicator of order flow toxicity, market instability, and market quality.

References

Abad, D, Massot, M., Pascual, R. 2018. Evaluating VPIN as a trigger for single-stock circuit breakers. *J. Bank. Finance* 86 (1), 21–36. doi.org/10.1016/j.jbankfin.2017.08.009

Abad, D, Yagüe, J., 2012. From PIN to VPIN: an introduction to order flow toxicity. *Spanish. R. of Fin. Econ.* 10 (2), 74–83. doi.org/10.1016/j.srfe.2012.10.002

Abreu, D., Brunnermeier. M. K., 2003. Bubbles and crashes. *Econometrica* 71 (1), 173–204. doi.org/10.1111/1468-0262.00393

Admati, A. R., Pfleiderer, P., 1988. A theory of intraday patterns: Volume and price variability. *R. of Financ. Stud.* 1 (1), 3–40. doi.org/10.1093/rfs/1.1.3

Andersen, T., Bondarenko, O., 2014a. VPIN and the flash crash. *J. Finan. Markets* 17 (Jan), 1–46. doi.org/10.1016/j.finmar.2013.05.005

Andersen, T., Bondarenko, O., 2014b. Reflecting on the VPIN dispute. *J. Finan. Markets* 17 (Jan), 53–64. doi.org/10.1016/j.finmar.2013.08.002

Aquilina, M., Budish, E., O'Neill, P. 2022. Quantifying the high-frequency trading "arms race". *Q. J. Economics* 137 (1), 493–564. doi.org/10.1093/qje/qjab032

Barber, B.M, Huang X., Odean, T. Schwarz, C. 2022. Attention-induced trading and returns: Evidence from Robinhood users. *J. Finance* 70 (6), 3141–3190. doi.org/10.1111/jofi.13183

Boehmer, E., Li, D., Saar, G., 2018. The competitive landscape of high-frequency trading firms. *Rev. Finan. Stud.* 31 (6), 2227-2276. doi.org/10.1093/rfs/hhx144

Breckenfelder, J., 2024. Competition among high-frequency traders and market quality. *J. Econ. Dyn. & Control* 166, 104922. doi.org/10.1016/j.jedc.2024.104922

Brogaard, J., Hendershott, T., Riordan, R., 2014. High-frequency trading and price discovery. *R. Finan. Stud.* 27 (8), 2267–2306. doi.org/10.1093/rfs/hhu032
Brunnermeier, M. K., Pedersen, L. H., 2005. Predatory trading. *J. Finance* 60 (4), 1825–1863. https://www.jstor.org/stable/3694855
Brunnermeier, M. K., Pedersen, L. H., 2009. Market liquidity and funding liquidity. *R. Finan. Stud.* 22 (6), 2201–2238. doi.org/10.1093/rfs/hhn098
Budish, E. B., Cramton, P. C., Kyle, A. S., Lee, J., Malec, D., 2023. *Flow trading*. NBER Working Paper 31098. doi.org/10.3386/w31098
Budish, E. B., Cramton, P. C., Shim J., 2015. The high-frequency trading arms race: Frequent batch auctions as a market design response. *Q. J. Econ.* 130 (4), 1547–1621. doi.org/10.1093/qje/qjv027
Chordia, T., Subrahmanyam, A., 2004. Order imbalance and individual stock returns: Theory and evidence. *J. Financ. Econ.* 72 (3), 485–518. doi.org/10.1016/S0304-405X(03)00175-2
Easley, D., Lopez de Prado, M., O'Hara, M., 2011a. The microstructure of the flash crash: Flow toxicity, liquidity crashes, and the probability of informed trading. *J. Port. Management* 37 (3), 118–128. doi.org/10.3905/jpm.2011.37.2.118
Easley, D., Lopez de Prado, M., O'Hara, M., 2011b. The exchange of flow toxicity. *J. Trading* 6, 8–13. doi.org/10.3905/jot.2011.6.2.008
Ellis, K., Michaely, R., O'Hara, M. 2000. The accuracy of trade classification rules: Evidence from Nasdaq. *J. Financ. Quant. Analysis* 35 (4), 529–551. doi.org/10.2307/2676254
Engle, R. F., Russel, J. R., 1998. Autoregressive conditional duration: A new model for irregularly spaced transaction data. *Econometrica* 66 (5), 1127–1162. doi.org/10.2307/2999632
Fama, E. 1998. Market efficiency, long-term returns, and behavioral finance. *J. Financ. Econ.* 49, 283–306. doi.org/10.1016/S0304-405X(98)00026-9
Fernandes, M., Grammig, J., 2006. A family of autoregressive conditional duration models. *J. Econometrics* 130 (1), 1–23. doi.org/10.1016/j.jeconom.2004.08.016
Filimonov, V., Wheatley, S., Sornette, D., 2015. Conditional duration point processes via mapping to the self-excited Hawkes process. *Commun Nonlinear Sci Numer Simulat* 22, 23–37. doi.org/10.1016/j.cnsns.2014.08.042
Hagströmer, B., Nordén, L. L., 2013. The diversity of high-frequency traders. *J. Financ. Markets* 16 (4), 741–770. doi.org/10.1016/j.finmar.2013.05.009
Haldane, A., 2011, *The race to zero*. Speech given at Int. Econ. Ass. Sixteenth World Congress, Beijing, China, 8 July. <https://www.bankofengland.co.uk/speech/2011/the-race-to-zero-speech-by-andy-haldane>. Accessed 6 Oct. 2023.
Harris, L., 1989. S&P 500 cash stock price volatilities, *J. Finance* 44 (5), 1155–1176. doi.org/10.1111/j.1540-6261.1989.tb02648.x
Hasbrouck, J., Saar, G., 2013. Low latency trading. *J. Financ. Markets* 16 (4), 646–679. doi.org/10.1016/j.finmar.2013.05.003
Hastie, T. J., Tibshirani, R. J., Friedman, J. H., 2009. *The Elements of Statistical Learning: Data Mining, Inference, and Prediction*. 2nd ed. New York: Springer-Verlag. <https://link.springer.com/book/10.1007/978-0-387-84858-7>. Accessed 13 Sept. 2013.
Hendershott, T, Livdan, D., Schürhoff, N., 2015. Are institutions informed about news? *J. Financ. Econ.* 117 (2), 249–287. doi.org/10.1016/j.jfineco.2015.03.007
Huang, J., Wang, J., 2009. Liquidity and market crashes. *R. Financ. Stud.* 22 (7), 2607–2643. doi.org/10.1093/rfs/hhn086
Ibrahim, B. M., Kalaitzoglou, I., 2016. Why do carbon prices and price volatility change? *J. Bank. Finance* 63 (2), 76–94. doi.org/10.1016/j.jbankfin.2015.11.004

Johnson N., Guannan, Z., Hunsader, E., Qi, H, Johnson, N., Meng, J., Tivnan, B., 2013. Abrupt rise of new machine ecology beyond human response time, *Sci. Rep.* 3, *Nature* 2627. doi.org/10.1038/srep02627

Judd, C. M., Kenny, D. A., 1981. Process analysis: Estimating mediation in treatment evaluations. *Evaluation Review* 5 (5), 602–619. doi.org/10.1177/0193841X8100500502.

Kyle, A. S. 1985. Continuous auctions and insider trading. *Econometrica* 53 (6), 1315–1335. doi.org/10.2307/1913210

Li, S., Wang, X., Ye, M., 2021. Who provides liquidity, and when? *J. of Financ. Econ.* 141 (3), 968–980. doi.org/10.1016/j.jfineco.2021.04.020

Linton, O., O'Hara, M., Zigrand, J-P., 2011. *The future of computer trading in financial markets*. Working paper. Foresight, Government Office for Science. <https://www.researchgate.net/publication/263888781>. Accessed 10 Nov. 2012.

Mackintsoh, P., 2020. *Who counts as a retail investor?* Nasdaq articles. <https://www.nasdaq.com/articles/who-counts-as-a-retail-investor-2020-12-17>. Accessed 5 October 2023.

Madhavan, A., 2000. Market microstructure: a survey. *J. Financ. Markets* 3 (3), 205–258. doi.org/10.1016/S1386-4181(00)00007-0

Madhavan, A., 2012. Exchange-traded funds, market structure, and the flash crash. *Financ. Analysts J.* 68 (4), 20–35. doi.org/10.2469/faj.v68.n4.6

Madhavan, A., M. Richardson, Roomans, M., 1997. Why do security prices change? A transaction-level analysis of NYSE stocks. *R. Financ. Stud.* 10 (4), 1035–1064. doi.org/10.1093/rfs/10.4.1035

O'Hara, M., 2015. High frequency market microstructure. *J. Financ. Econ.* 116 (2), 257–270. doi.org/10.1016/j.jfineco.2015.01.003

Sarkar, A., Schwartz, R. A., 2009. Market sidedness: Insights into motives for trade initiation. *J. Finance* 64 (1), 375–423. doi.org/10.1111/j.1540-6261.2008.01437.x

Sobel, M. E., 1982. Asymptotic confidence intervals for indirect effects in structural equation models. *Sociological Methodology* 13 (1), 290–312. doi.org/10.2307/270723

Stein, J., 2009. Presidential address: Sophisticated investors and market efficiency. *J. Finance* 64 (4), 1517–1548. doi.org/10.1111/j.1540-6261.2009.01472.x

Tkatch, I., Kandel, E., 2004. *Demand for Immediacy: Time is Money*. Maurice Falk Institute for Economic Research in Israel. <https://pages.stern.nyu.edu/~rengle/Tkatch-F2004.pdf>. Accessed 5 Jan. 2023.

U.S. Commodity Futures Trading Commission and U.S. Securities and Exchange Commission, 2010, *Findings Regarding The Market Events of May 6, 2010*. <https://www.sec.gov/files/marketevents-report.pdf>. Accessed 15 May 2023.

Welch, I. 2022. The wisdom of the Robinhood crowd. *J. Finance* 77 (3), 1489–1527. doi.org/10.1111/jofi.13128

Yadav, Y., 2015. How algorithmic trading undermines efficiency in capital markets. *Vanderbilt Law Rev.* 68 (6), 1607–1671. <https://scholarship.law.vanderbilt.edu/vlr/vol68/iss6/3/>. Accessed 18 Nov. 2024.

Yao, C., Ye, M., 2018. Why trading speed matters: A tale of queue rationing under price controls. *Rev. Finan. Stud.* 31 (6), 2157–2183. doi.org/10.1093/rfs/hhy002

Table 1 Descriptive statistics, estimation results, and mispricing graphs

This table has two panels and two graphs. Panel A presents descriptive statistics of returns (R), quantity (Q), duration (D), and the average overreaction and underreaction in the next 5, 15, and 25 transactions (AOU5, AOU15, AOU25) for the full sample and for algorithmic, retail, and institutional trades separately. Panel B presents the estimation results of Equations (2)-(6) and the hazard function (Equation B.2.1 in online Appendix B). Graph 1 plots AOU15 over levels of the Surprise in Arbitrage Capacity (*SAC*). Graph 2 plots the standard deviation of mispricing over different numbers of prospective transactions. The inset table in Graph 2 presents the standard deviation (std) of mispricing in bins of prospective transactions, *F*-test values on the *incremental* dissipation in the square of std from one bin to the next from left to right, its *p*-value (p), and the average (a) and median (m) times in minutes of the transaction bins.

Panel A		R	Q	D	AOU5	AOU15	AOU25		R	Q	D	AOU5	AOU15	AOU25
Avg.	Full Sample	0.00	205.8	0.90	0.00	0.00	0.00	Algorithmic	0.00	128.66	0.12	0.00	0.00	0.00
Min.	230,084,293	-52.66	1	0.00	-55.66	-11.32	-9.02	168,237,635	-230.21	1	0.00	-30.46	-39.90	-39.13
Max.		52.65	88000	4500	47.05	8.35	6.40	(73.12%)	195.57	1378	0.65	92.11	78.73	55.31
Std.		0.17	538.94	2.34	1.03	0.82	0.74		0.08	168.73	0.17	1.53	1.64	0.97
Avg.	Retail	0.00	155.28	2.37	0.00	0.00	0.00	Institutional	0.00	2377.23	0.47	0.00	0.00	0.00
Min.	54,264,480	-37.02	1	0.65	-34.07	-27.33	-22.75	7,582,178	-22.75	796	0.00	-26.43	-30.16	-11.62
Max.	(23.58%)	36.08	2789	7100	43.50	28.85	24.76	(3.30%)	24.76	88100	6900	3.45	32.35	20.89
Std.		0.07	180.34	4.16	0.97	0.64	0.48		0.05	2513.48	3.62	0.75	0.64	0.39

Panel B	θ1	θ2	θ3	φ0	φ1	φ2	φ3	ρ	$\sigma\varepsilon^2$	$\sigma\xi^2$	ω	α	β	γ1	γ2	γ3	g1	g2	s1	s2
Avg.	0.0076	0.0054	0.0054	0.0094	-0.004	-0.003	-0.0031	0.34	0.32	0.04	0.0263	0.269	0.7243	0.9529	3.6529	0.3641	3.17	1.87	0.89	2.97
Med.	0.0043	0.0022	0.0036	0.0078	-0.0022	-0.0011	-0.0018	0.34	0.14	0.02	0.0216	0.2404	0.7529	0.9231	2.7225	0.3678	2.02	1.16	0.99	3.23
S.error	0.0001	0.0001	0.0001	0.0001	0.0001	0.0001	0.0001	0.00	0.01	0.08	0.0002	0.0019	0.0007	0.0123	0.027	0.0022	0.06	0.08	0.02	0.19
Std.	0.0143	0.0097	0.0061	0.0053	0.0086	0.0057	0.0054	0.14	0.60	0.07	0.0162	0.1103	0.1103	0.0564	2.9563	0.0564	3.43	2.16	0.23	0.92

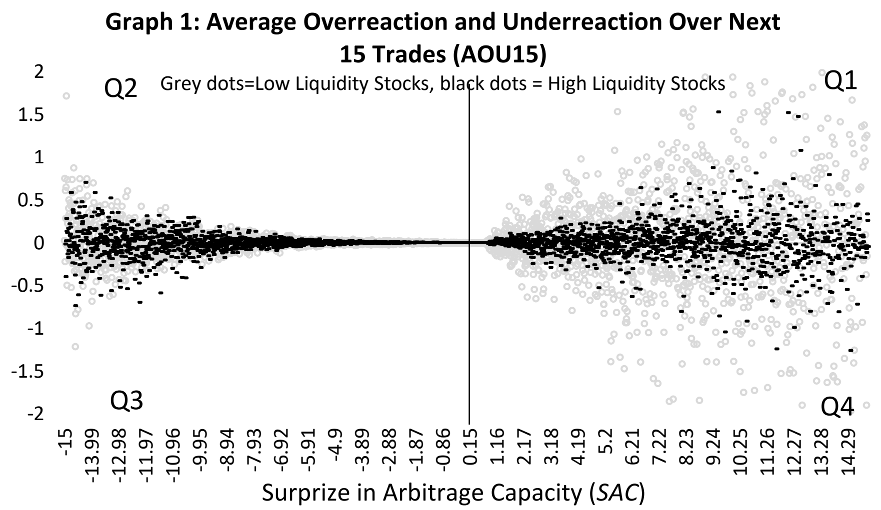

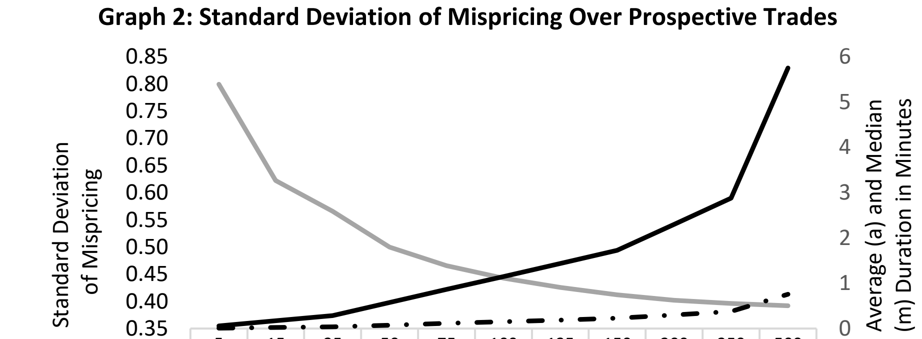

	5	15	25	50	75	100	125	150	200	250	500
std	0.80	0.62	0.57	0.50	0.47	0.44	0.43	0.41	0.40	0.40	0.39
F-test	1.28	1.10	1.13	1.07	1.05	1.04	1.03	1.03	1.02	1.01	
(p)	(0.00)	(0.00)	(0.00)	(0.00)	(0.01)	(0.02)	(0.06)	(0.10)	(0.22)	(0.31)	
minutes (a)	0.06	0.17	0.29	0.58	0.86	1.15	1.44	1.73	2.30	2.88	5.75
minutes (m)	0.01	0.02	0.04	0.08	0.11	0.15	0.19	0.23	0.30	0.38	0.76

Table 2 Mispricing in quartiles of AOU15 against surprise in arbitrage capacity

This table has six panels separated by full horizontal lines. The top three panels present slope estimates (*t*-stats in parenthesis) and R^2 of regressions of mispricing on the surprise in arbitrage capacity (*SAC*) in quadrants Q1-Q4 of Graph 1 in Table 1. This is presented for All trades (top panel) and for trades of Low liquidity and High Liquidity stocks (second two panels). The bottom three panels present values of a *t*-test on the difference in slopes across quadrants as tests of asymmetries (*p*-values in parenthesis). The critical values of the *t*-stats at 10%, 5%, and 1% are 1.29, 1.66, and 2.36, respectively.

		Full Sample	News			Agent Type		
	Quadrant	All	Good	No	Bad	Algorithmic	Institutional	Retail
All	Q1	0.0522	0.0405	0.0531	0.0738	0.0637	0.0411	0.0517
		(87.19)	(32.99)	(52.34)	(19.14)	(91.50)	(83.84)	(68.23)
	Q2	-0.0443	-0.0517	-0.0389	-0.0537	-0.0596	-0.0227	-0.0462
		(-81.60)	(-90.88)	(-92.08)	(-84.09)	(-92.27)	(-55.90)	(-71.63)
	Q3	0.0456	0.0544	0.0397	0.0573	0.0616	0.0276	0.0495
		(71.50)	(84.41)	(87.16)	(80.06)	(81.57)	(52.32)	(62.61)
	Q4	-0.0574	-0.0481	-0.0593	-0.0742	-0.0709	-0.0428	-0.0586
		(-76.62)	(-25.77)	(-46.46)	(-19.21)	(-60.44)	(-71.24)	(-68.18)
	R^2	0.3131	0.3519	0.3016	0.3992	0.4625	0.4264	0.4570
Low Liquidity	Q1	0.1035	0.0658	0.1057	0.1342	0.1393	0.0641	0.1072
		(29.76)	(26.58)	(29.79)	(28.81)	(36.33)	(36.30)	(16.65)
	Q2	-0.0516	-0.0796	-0.0456	-0.0743	-0.0643	-0.0368	-0.0538
		(-85.38)	(-71.17)	(-59.61)	(-67.13)	(-79.01)	(-32.50)	(-84.64)
	Q3	0.0554	0.0766	0.0472	0.0767	0.0813	0.0221	0.0628
		(83.40)	(71.06)	(54.56)	(62.65)	(82.59)	(65.56)	(82.04)
	Q4	-0.1215	-0.0683	-0.1317	-0.1509	-0.1531	-0.0990	-0.1125
		(-39.91)	(-28.21)	(-27.25)	(-25.14)	(-44.62)	(-44.59)	(-30.52)
High Liquidity	Q1	-0.0683	-0.0352	-0.0786	-0.0824	-0.0946	-0.0933	-0.0170
		(-30.01)	(-15.48)	(-27.25)	(-23.89)	(-29.45)	(-18.09)	(-42.48)
	Q2	0.0313	0.0242	0.0280	0.0369	0.0333	0.0344	0.0261
		(50.26)	(42.31)	(34.08)	(24.94)	(73.25)	(7.56)	(69.97)
	Q3	-0.0374	-0.0244	-0.0291	-0.0325	-0.0674	-0.0072	-0.0377
		(-50.07)	(-41.53)	(31.22)	(-16.71)	(-59.32)	(-8.01)	(-32.88)
	Q4	0.0797	0.0471	0.0893	0.0809	0.0202	0.0201	0.0182
		(35.46)	(24.05)	(20.87)	(22.24)	(24.34)	(24.26)	(57.78)
	R^2	0.3828	0.4089	0.3747	0.4560	0.4630	0.4619	0.4603
All	Q1 vs Q4	-3.90	-2.46	-2.71	-0.05	-3.86	-1.55	-4.24
		(0.00)	(0.01)	(0.00)	(0.48)	(0.00)	(0.06)	(0.00)
	Q2 vs Q3	-1.07	-2.20	-0.92	-2.67	-1.43	-5.20	-2.33
		(0.14)	(0.01)	(0.18)	(0.00)	(0.08)	(0.00)	(0.01)
	Q1 vs Q2	6.87	-6.26	9.87	4.46	3.05	20.50	3.96
		(0.00)	(0.00)	(0.00)	(0.00)	(0.00)	(0.00)	(0.00)
	Q4 vs Q3	8.53	-2.50	11.31	3.67	4.82	13.50	5.49
		(0.00)	(0.01)	(0.00)	(0.00)	(0.00)	(0.00)	(0.00)
Low Liquidity	Q1 vs Q4	-2.76	-0.51	-3.10	-1.57	-1.90	-8.76	-0.52
		(0.00)	(0.30)	(0.00)	(0.06)	(0.03)	(0.00)	(0.30)
	Q2 vs Q3	-2.95	1.37	-1.00	-1.00	-9.45	10.01	-6.39
		(0.00)	(0.09)	(0.16)	(0.16)	(0.00)	(0.00)	(0.00)
	Q1 vs Q2	12.71	-3.85	13.94	10.38	16.13	9.42	7.55
		(0.00)	(0.00)	(0.00)	(0.00)	(0.00)	(0.00)	(0.00)
	Q4 vs Q3	17.83	-2.38	14.82	10.27	16.26	30.08	11.17
		(0.00)	(0.01)	(0.00)	(0.00)	(0.00)	(0.00)	(0.00)
High Liquidity	Q1 vs Q4	-0.60	1.03	-0.98	-1.02	-7.80	-4.16	-0.37
		(0.28)	(0.15)	(0.16)	(0.15)	(0.00)	(0.00)	(0.35)
	Q2 vs Q3	0.92	0.96	-0.34	-1.16	5.04	-1.80	0.91
		(0.18)	(0.17)	(0.37)	(0.12)	(0.00)	(0.04)	(0.18)
	Q1 vs Q2	5.13	-8.74	2.58	2.92	3.72	2.75	8.10
		(0.00)	(0.00)	(0.00)	(0.00)	(0.00)	(0.00)	(0.00)
	Q4 vs Q3	3.56	-5.14	2.69	2.02	18.64	7.40	11.72
		(0.00)	(0.00)	(0.00)	(0.02)	(0.00)	(0.00)	(0.00)

Table 3 Asymmetries in mispricing uncertainty

This table presents values of an *F*-test (*p*-value in parentheses) in *SAC* bins on the variance ratio between positive and negative *SAC* (Panel A), low and high liquidity stocks (Panel B), and types of news and agent (Panel C).

Panel A																
	|*SAC*|	All		Good News		No News		Bad News		Algorithmic		Institutional		Retail	
All	1-3	21.98	(0.00)	6.42	(0.00)	19.88	(0.00)	7.12	(0.00)	9.27	(0.00)	0.99	(0.59)	3.91	(0.00)
	3-5	14.91	(0.00)	4.22	(0.00)	12.20	(0.00)	6.13	(0.00)	7.86	(0.00)	1.16	(0.01)	5.38	(0.00)
	5-7	8.11	(0.00)	1.82	(0.00)	6.57	(0.00)	3.31	(0.00)	6.95	(0.00)	1.11	(0.05)	5.96	(0.00)
	7-9	4.27	(0.00)	0.93	(0.83)	3.52	(0.00)	1.86	(0.00)	4.34	(0.00)	1.15	(0.01)	4.30	(0.00)
	9-11	2.45	(0.00)	0.78	(0.99)	1.95	(0.00)	1.55	(0.00)	2.87	(0.00)	0.50	(1.00)	2.32	(0.00)
	11-13	1.67	(0.00)	0.80	(0.93)	1.40	(0.00)	1.26	(0.11)	1.61	(0.00)	1.17	(0.01)	1.56	(0.00)
	13-15	1.07	(0.19)	0.67	(0.98)	1.02	(0.39)	0.93	(0.60)	1.48	(0.00)	0.71	(1.00)	1.14	(0.02)
Low Liquidity	1-3	22.55	(0.00)	6.23	(0.00)	20.52	(0.00)	6.99	(0.00)	14.71	(0.00)	0.84	(1.00)	4.35	(0.00)
	3-5	16.15	(0.00)	4.20	(0.00)	13.42	(0.00)	6.26	(0.00)	9.50	(0.00)	1.25	(0.00)	5.87	(0.00)
	5-7	9.71	(0.00)	1.88	(0.00)	8.03	(0.00)	3.37	(0.00)	8.28	(0.00)	0.84	(1.00)	7.53	(0.00)
	7-9	5.13	(0.00)	0.97	(0.60)	4.21	(0.00)	1.92	(0.00)	4.81	(0.00)	1.15	(0.01)	5.53	(0.00)
	9-11	2.84	(0.00)	0.73	(0.99)	2.34	(0.00)	1.65	(0.00)	4.05	(0.00)	0.99	(0.56)	2.93	(0.00)
	11-13	1.95	(0.00)	0.83	(0.81)	1.73	(0.00)	1.36	(0.07)	1.92	(0.00)	1.12	(0.04)	2.04	(0.00)
	13-15	1.28	(0.01)	0.77	(0.84)	1.28	(0.02)	0.95	(0.55)	1.76	(0.00)	0.68	(1.00)	1.32	(0.00)
High Liquidity	1-3	17.17	(0.00)	12.63	(0.00)	14.84	(0.00)	4.09	(0.00)	9.93	(0.00)	0.54	(1.00)	4.74	(0.00)
	3-5	11.09	(0.00)	6.04	(0.00)	8.80	(0.00)	0.61	(0.95)	6.37	(0.00)	1.08	(0.11)	6.59	(0.00)
	5-7	4.23	(0.00)	2.08	(0.00)	3.59	(0.00)	0.36	(1.00)	4.36	(0.00)	1.29	(0.00)	4.09	(0.00)
	7-9	2.17	(0.00)	1.18	(0.07)	1.93	(0.00)	0.21	(1.00)	3.25	(0.00)	1.16	(0.01)	3.13	(0.00)
	9-11	1.51	(0.00)	1.79	(0.00)	1.22	(0.01)	0.14	(1.00)	1.65	(0.00)	0.97	(0.71)	1.75	(0.00)
	11-13	1.25	(0.01)	1.50	(0.02)	1.04	(0.37)	0.12	(1.00)	1.22	(0.00)	1.23	(0.00)	1.18	(0.00)
	13-15	0.84	(0.91)	0.33	(1.00)	0.92	(0.72)	0.34	(0.79)	0.93	(0.88)	0.17	(1.00)	1.24	(0.00)

Panel B	Low versus High Liquidity Stocks													
SAC	All		Good News		No News		Bad News		Algorithmic		Institutional		Retail	
-15--13	2.94	(0.00)	2.94	(0.00)	3.25	(0.00)	3.14	(0.02)	5.18	(0.00)	1.39	(0.00)	5.56	(0.00)
-13--11	2.17	(0.00)	2.73	(0.00)	2.51	(0.00)	1.43	(0.22)	4.57	(0.00)	1.19	(0.00)	2.02	(0.00)
-11--9	1.59	(0.00)	3.08	(0.00)	1.60	(0.00)	1.96	(0.00)	3.33	(0.00)	1.11	(0.05)	2.52	(0.00)
-9--7	1.60	(0.00)	2.61	(0.00)	1.66	(0.00)	1.54	(0.00)	3.34	(0.00)	1.11	(0.05)	1.27	(0.00)
-7--5	1.49	(0.00)	2.08	(0.00)	1.52	(0.00)	1.06	(0.19)	3.27	(0.00)	1.09	(0.09)	4.29	(0.00)
-5--3	2.27	(0.00)	2.69	(0.00)	2.23	(0.00)	1.00	(0.53)	6.38	(0.00)	2.13	(0.00)	1.63	(0.00)
-3--1	3.04	(0.00)	4.07	(0.00)	2.95	(0.00)	1.43	(0.00)	8.51	(0.00)	2.84	(0.00)	1.90	(0.00)
-1-1	4.95	(0.00)	6.35	(0.00)	4.41	(0.00)	3.98	(0.00)	5.09	(0.00)	1.70	(0.00)	2.86	(0.00)
1-3	4.00	(0.00)	2.00	(0.00)	4.11	(0.00)	2.44	(0.00)	7.33	(0.00)	2.60	(0.00)	2.95	(0.00)
3-5	3.32	(0.00)	1.86	(0.00)	3.42	(0.00)	10.20	(0.00)	5.15	(0.00)	1.89	(0.00)	2.27	(0.00)
5-7	3.43	(0.00)	1.88	(0.00)	3.39	(0.00)	9.80	(0.00)	5.70	(0.00)	2.01	(0.00)	1.92	(0.00)
7-9	3.78	(0.00)	2.15	(0.00)	3.67	(0.00)	13.97	(0.00)	7.45	(0.00)	1.96	(0.00)	1.27	(0.00)
9-11	2.99	(0.00)	1.24	(0.16)	3.05	(0.00)	23.59	(0.00)	10.34	(0.00)	1.86	(0.00)	2.59	(0.00)
11-13	3.38	(0.00)	1.51	(0.08)	4.17	(0.00)	15.97	(0.00)	14.72	(0.00)	2.06	(0.00)	2.45	(0.00)
13-15	4.50	(0.00)	6.96	(0.00)	4.55	(0.00)	8.70	(0.05)	15.68	(0.00)	1.48	(0.00)	4.08	(0.00)

Panel C	Type of News						Type of Agent					
SAC	Bad/Good		Bad/No		Good/No		Algo/Institutional		Algo/Retail		Retail/Institutional	
-15--13	1.37	(0.00)	1.42	(0.00)	1.04	(0.27)	1.48	(0.00)	7.15	(0.00)	1.42	(0.00)
-13--11	1.27	(0.00)	1.80	(0.00)	1.42	(0.00)	1.61	(0.00)	2.37	(0.00)	1.74	(0.00)
-11--9	1.25	(0.00)	2.43	(0.00)	1.95	(0.00)	2.87	(0.00)	4.46	(0.00)	1.85	(0.00)
-9--7	1.20	(0.00)	2.76	(0.00)	2.31	(0.00)	3.34	(0.00)	5.05	(0.00)	1.58	(0.00)
-7--5	1.29	(0.00)	2.77	(0.00)	2.15	(0.00)	2.95	(0.00)	7.80	(0.00)	0.86	(0.99)
-5--3	1.32	(0.00)	2.68	(0.00)	2.03	(0.00)	3.86	(0.00)	5.80	(0.00)	1.66	(0.00)
-3--1	1.24	(0.00)	2.49	(0.00)	2.01	(0.00)	4.27	(0.00)	6.54	(0.00)	1.29	(0.00)
-1-1	1.35	(0.00)	2.67	(0.00)	1.98	(0.00)	3.20	(0.00)	7.26	(0.00)	0.70	(1.00)
1-3	1.37	(0.00)	0.89	(1.00)	0.65	(1.00)	1.09	(0.08)	2.78	(0.00)	1.27	(0.00)
3-5	1.92	(0.00)	1.34	(0.00)	0.70	(1.00)	3.27	(0.00)	4.60	(0.00)	1.07	(0.14)
5-7	2.34	(0.00)	1.40	(0.00)	0.60	(1.00)	6.17	(0.00)	7.34	(0.00)	1.95	(0.00)
7-9	2.40	(0.00)	1.46	(0.00)	0.61	(1.00)	7.01	(0.00)	6.79	(0.00)	1.88	(0.00)
9-11	2.48	(0.00)	1.94	(0.00)	0.78	(0.98)	6.23	(0.00)	8.30	(0.00)	2.93	(0.00)
11-13	1.99	(0.00)	1.61	(0.01)	0.81	(0.90)	7.03	(0.00)	12.95	(0.00)	1.60	(0.00)
13-15	1.88	(0.01)	1.28	(0.13)	0.68	(0.97)	7.29	(0.00)	11.00	(0.00)	1.72	(0.00)

Table 4 The predictive power of the crowdedness of a trade

This table reports estimation results of the regression $Q_{i+s} = c + a|Crowd| + CV_i + u_i + e_i$, where Q = (*UHF*, *Algo.*, *runs*, *institutional*, *trade/order ratio*, *spread*)', CV = (*duration*, *volume*, *order count*, *sum of volume at best bid and best ask*)' are control variables, u are company fixed effects, and e are errors. The estimation is over $s = (5, 25, 50, 100, 150)'$ prospective transactions over the full sample. Results on control variables and fixed effects are not reported for brevity. Three separate regressions for each Q are reported in each panel separated by a full horizontal line. The first two rows in each panel report regression results with |*Crowd*| as an independent variable. The next 4 rows report regression results with signed *Crowd* (+ and –) with $t_{(+)\text{-}|\text{-}|}$ being a *t*-test (*p*-value in parentheses) of the difference in coefficients between *Crowd* + and *Crowd* -. The next 4 rows are results of regressions that dissect the coefficient $a \coloneqq (1-G)a^- + Ga^+$ with a smooth transition function $G = \left(1 + exp(-g(|Crowd| - Threshold))\right)^{-1}$, where a^- is the coefficient when $|Crowd| < Threshold$ and a^+ is the coefficient when $|Crowd| \geq Threshold$. The parameters: $threshold$, a^-, a^+, and g, are estimated with maximum likelihood assuming Normal errors. R^2 is reported for each regression. *t*-stats critical values are 1.29, 1.66, and 2.36 at 10%, 5%, and 1%.

		5	25	50	100	150		5	25	50	100	150
|*Crowd*|	UHF (% of trades x 1000)	0.3350	0.3127	0.2929	0.2675	0.2463	Algorithmic trading (% of trades)	0.6542	0.5880	0.4793	0.4255	0.3962
		(32.86)	(9.48)	(8.20)	(5.12)	(3.76)		(66.23)	(17.56)	(9.89)	(5.51)	(3.87)
R^2		0.1869	0.1163	0.0745	0.0614	0.0525		0.2363	0.1297	0.1135	0.0921	0.0785
Crowd+		0.3266	0.2980	0.2759	0.2530	0.2415		0.9274	0.6332	0.5073	0.4226	0.3837
		(24.26)	(9.16)	(5.86)	(3.67)	(2.80)		(90.38)	(19.17)	(10.15)	(5.45)	(3.78)
Crowd-		-0.3278	-0.3274	-0.2981	-0.2728	-0.2457		-0.5734	-0.5428	-0.4963	-0.4449	-0.4160
		(-23.64)	(-9.81)	(-6.14)	(-3.84)	(-2.76)		(-42.07)	(-15.95)	(-9.63)	(-5.57)	(-3.97)
R^2		0.2369	0.1202	0.1347	0.1074	0.1047		0.3542	0.1320	0.1213	0.1035	0.1024
t(+)-|-|		-0.04	-0.45	-0.23	-0.14	-0.02		14.82	1.35	0.11	-0.14	-0.16
		(0.48)	(0.33)	(0.41)	(0.44)	(0.49)		(0.00)	(0.09)	(0.46)	(0.44)	(0.44)
Threshold		0.0633	0.0548	0.0540	0.0521	0.0496		0.0628	0.0545	0.0511	0.0512	0.0465
		(1.94)	(2.18)	(2.39)	(3.06)	(3.93)		(1.76)	(2.00)	(2.57)	(3.09)	(4.09)
a^-		0.5863	0.5472	0.5126	0.4681	0.4310		1.1448	1.0290	0.8387	0.7447	0.6934
		(57.51)	(16.60)	(14.36)	(8.95)	(6.59)		(115.90)	(30.73)	(17.31)	(9.65)	(6.78)
a^+		0.0838	0.0782	0.0732	0.0669	0.0616		0.1635	0.1470	0.1198	0.1064	0.0991
		(8.22)	(2.37)	(2.05)	(1.28)	(0.94)		(16.56)	(4.39)	(2.47)	(1.38)	(0.97)
g		3.8520	3.1120	2.8629	2.6814	2.6447		2.3500	2.1608	1.9357	1.8330	1.7523
		(22.49)	(20.22)	(16.57)	(16.20)	(15.84)		(39.19)	(34.11)	(22.69)	(21.72)	(12.38)
|*Crowd*|	Intensity of runs (% of trades in a run)	0.7793	0.3861	0.3394	0.3229	0.3249	Institutional trading (% of trades)	0.3211	0.2715	0.2784	0.2678	0.2560
		(23.94)	(4.40)	(2.44)	(1.41)	(1.03)		(11.05)	(11.65)	(7.68)	(4.61)	(3.31)
R^2		0.1794	0.1261	0.1231	0.1094	0.0973		0.1194	0.0930	0.0825	0.0643	0.0580
Crowd+		0.9179	0.3515	0.2940	0.2706	0.2701		0.1619	0.2521	0.2450	0.2281	0.2160
		(28.54)	(4.07)	(2.15)	(1.20)	(0.87)		(17.94)	(10.98)	(6.95)	(4.10)	(2.93)
Crowd-		-0.6408	-0.4206	-0.3849	-0.3753	-0.3796		-0.2039	-0.2909	-0.3052	-0.2932	-0.2801
		(-19.34)	(-4.73)	(-2.73)	(-1.61)	(-1.19)		(-4.17)	(-12.31)	(-8.41)	(-5.12)	(-3.69)
R^2		0.2031	0.1321	0.1276	0.1199	0.0977		0.1584	0.1084	0.1009	0.0951	0.0820
t(+)-|-|		4.24	-0.39	-0.33	-0.23	-0.17		-6.72	-0.83	-0.84	-0.58	-0.43
		(0.00)	(0.35)	(0.37)	(0.41)	(0.43)		(0.00)	(0.20)	(0.20)	(0.28)	(0.33)
Threshold		0.0635	0.0514	0.0476	0.0501	0.0479		0.0627	0.0526	0.0498	0.0490	0.0457
		(1.66)	(2.03)	(2.48)	(3.23)	(4.05)		(1.94)	(2.10)	(2.45)	(3.16)	(3.97)
a^-		1.3639	0.6756	0.5940	0.5651	0.5685		0.5620	0.4750	0.4873	0.4686	0.4480
		(41.90)	(7.70)	(4.27)	(2.46)	(1.80)		(19.34)	(20.38)	(13.44)	(8.06)	(5.79)
a^+		0.1948	0.0965	0.0849	0.0807	0.0812		0.0803	0.0679	0.0696	0.0669	0.0640
		(5.99)	(1.10)	(0.61)	(0.35)	(0.26)		(2.76)	(2.91)	(1.92)	(1.15)	(0.83)
g		3.3246	2.8067	2.2790	2.0867	2.0452		1.1852	0.9873	0.9218	0.8924	0.6557
		(19.95)	(15.13)	(13.28)	(12.47)	(11.78)		(8.49)	(7.26)	(6.86)	(5.58)	(5.32)
|*Crowd*|	Trade-to-order ratio (% of trades/orders)	0.2657	0.1870	0.1732	0.1663	0.1624	Bid-ask spread ($)	0.1537	0.1613	0.1690	0.1740	0.1778
		(51.04)	(8.66)	(4.39)	(2.29)	(1.54)		(38.24)	(13.00)	(47.64)	(51.14)	(53.52)
R^2		0.3015	0.2612	0.2423	0.2279	0.2032		0.3209	0.2513	0.1961	0.1697	0.1560
Crowd+		0.1719	0.1075	0.1000	0.0980	0.0987		0.1158	0.1419	0.1471	0.1519	0.1557
		(33.69)	(5.08)	(2.59)	(1.38)	(0.93)		(43.67)	(11.62)	(6.29)	(3.38)	(2.37)
Crowd-		-0.3595	-0.2666	-0.2464	-0.2346	-0.2261		-0.1742	-0.1808	-0.1850	-0.1906	-0.1944
		(-68.39)	(-12.24)	(-6.19)	(-3.20)	(-2.14)		(-63.79)	(-14.37)	(-7.67)	(-4.12)	(-2.87)
R^2		0.3812	0.2724	0.2537	0.2302	0.2153		0.3578	0.2773	0.2037	0.1744	0.1625
t(+)-|-|		-18.10	-3.71	-1.87	-0.94	-0.60		-10.85	-1.57	-0.80	-0.42	-0.29
		(0.00)	(0.00)	(0.03)	(0.17)	(0.27)		(0.00)	(0.06)	(0.21)	(0.34)	(0.39)
Threshold		0.0632	0.0554	0.0533	0.0527	0.0512		0.0632	0.0536	0.0526	0.0502	0.0495
		(1.84)	(2.20)	(2.36)	(3.12)	(4.00)		(1.97)	(2.20)	(2.46)	(3.06)	(4.06)
a^-		0.4650	0.3273	0.3031	0.2911	0.2842		0.2690	0.2823	0.2957	0.3046	0.3112
		(89.32)	(15.15)	(7.68)	(4.00)	(2.69)		(66.93)	(22.74)	(83.37)	(89.50)	(93.66)
a^+		0.0664	0.0468	0.0433	0.0416	0.0406		0.0384	0.0403	0.0422	0.0435	0.0445
		(12.76)	(2.16)	(1.10)	(0.57)	(0.38)		(9.56)	(3.25)	(11.91)	(12.79)	(13.38)
g		2.0582	1.7567	1.6693	1.4008	1.3770		4.3385	3.4929	3.0794	2.8652	2.8081
		(38.59)	(35.39)	(20.63)	(9.64)	(6.34)		(29.89)	(25.78)	(18.57)	(16.71)	(16.40)

Table 5 The predictive power of crowdedness in interval measures

This table presents estimation results of: $UHF_t = c + aVPIN_t + \beta \sum_{trades_t} |Crowd| + \gamma Algo_t + \delta Inst_t + \boldsymbol{\varepsilon}(Algo_t \times \sum_{trades_t} |Crowd|, Algo_t \times \sum_{trades_t} |Crowd|)' + \boldsymbol{\zeta} CV_t + u_t + e_t$. "Level" and "Lag" in the column headings refer to contemporaneous and t+1 forecast estimates, respectively. t indexes the time $interval = (5'', 30'', 1', 5', 30', 60')'$; *UHF*, *Algo.*, *and Inst.* are the numbers of trades classified as UHF events, algorithmic, or institutional per stock per interval; *CV* = (conditional variance of Δp_t (*C.Var.*), *bid-ask spread*, *trade/order ratio*, *duration*, *volume*)$'$ is a set of control variables averaged over interval t (only *C.Var.* is reported for brevity); u_t are fixed effects. The first column in each panel is an all-parameter estimation, with (t-stats; *variance inflation factor*) in parentheses. The second column presents a LASSO estimation (Hastie et al., 2009) using the BIC criteria for variable selection and 70% of sample for training, with (t-stats) in parentheses. The bottom three rows in each panel report the R^2 and the estimates of the overall indirect (*Ind.*) impact of *Crowd* on UHF (Judd and Kenny, 1981) and separately for *VPIN* (*V*) and for *Algo*. (*A*) (Sobel, 1982). Parentheses in the second column next to *Ind.* values and below $V \mid A$ values contain (2.5%; 97.5%) confidence intervals based on 5000 bootstraps.

		5 Level	LASSO	5 Lag	LASSO	30 Level	LASSO	30 Lag	LASSO	60 Level	LASSO	60 Lag	LASSO
Seconds $''$	*VPIN*	0.2266	0.2173	0.2079		0.0243	0.0355	0.1120		0.0519		0.1763	
		(13.73; 2.9)	(10.16)	(12.68; 1.4)		(0.93; 3.1)	(7.75)	(4.28; 2.3)		(1.67; 4.1)		(5.68; 4.9)	
	$\lvert$*Crowd*$\rvert$	0.1532	0.0609	0.1808	0.3289	0.2034	0.2099	0.0645	0.1766	0.2305	0.3950	0.2912	0.2843
		(10.38; 1.2)	(87.22)	(12.32; 1.2)	(16.48)	(7.65; 1.4)	(61.39)	(2.94; 1.3)	(7.92)	(7.20; 1.5)	(46.09)	(1.92; 1.4)	(7.77)
	Algo.	0.0813		0.0857		-0.0459		-0.0627		-0.0529		-0.2456	
		(7.32; 1.5)		(7.55; 1.4)		(-2.52; 1.7)		(-3.77; 1.9)		(-3.23; 1.8)		(-7.99; 2.1)	
	$\lvert$*Crowd*$\rvert$x*Algo*	0.0310	0.1037	0.0028		0.0150	0.0200	0.0231		0.0104	0.1846	0.0104	
		(10.20; 1.5)	(6.53)	(10.59; 1.5)		(10.99; 2.4)	(12.48)	(15.36; 2.4)		(13.42; 7.0)	(19.89)	(14.34; 7.0)	
	$\lvert$*Crowd*$\rvert$x*VPIN*	0.0832	0.1237	0.0410		0.0375	0.0489	0.0690		0.0214	0.2124	0.0314	
		(14.36; 1.5)	(8.00)	(17.12 1.5)		(19.07; 2.4)	(25.80)	(35.13; 2.4)		(16.62; 7.0)	(32.55)	(25.91; 7.0)	
	Inst.	-0.0781		-0.0364		-0.0417		-0.0280		-0.0447		-0.0822	
		(-1.54; 1.5)		(-1.28; 1.4)		(-0.47; 1.8)		(-0.03; 1.6)		(-0.37; 1.8)		(-0.67; 1.7)	
	C. Var.	0.1253	0.1248	0.0762	0.0884	0.0812	0.0809	0.0458	0.0413	0.0615	0.0613	0.0342	0.0462
		(429.3; 1.0)	(427.95)	(262.6; 1.0)	(231.70)	(308.5; 1.0)	(307.76)	(174.2; 2.0)	(150.16)	(243.3; 1.0)	(242.87)	(135.2; 1.0)	(128.18)
	R^2	0.3747	0.2777	0.2111	0.1621	0.4811	0.3021	0.3106	0.2839	0.4254	0.2792	0.3272	0.2222
	Ind.	0.0577	(0.04; 0.08)	0.0428	(0.03; 0.05)	0.3549	(0.15; 0.82)	0.4636	(0.11; 0.87)	0.4533	(0.19; .93)	0.6647	(0.17; 0.95)
	$V \mid A$	0.0412	0.0167	0.0301	0.0130	0.2982	0.0567	0.4188	0.0448	0.3864	0.0669	0.6201	0.0451
		(0.03; 0.07)	(0.01; 0.03)	(0.01; 0.04)	(0.01; 0.2)	(0.13; 0.69)	(0.03 0.17)	(0.14; 0.69)	(0.01; 0.18)	(0.17; 0.88)	(0.03; 0.15)	(0.15; 1.36)	(0.01; 0.17)
Minutes $'$	*VPIN*	0.0483		0.0741		0.0261		-0.1390		0.0098		-0.1882	
		(1.19; 4.7)		(1.76; 5.2)		(0.68; 8.2)		(-1.92; 8.3)		(0.87; 9.3)		(-1.15; 9.7)	
	$\lvert$*Crowd*$\rvert$	0.7490	0.7239	0.2793	0.2681	0.8041	1.1666	0.4712	0.7092	0.6869	0.4558	0.2495	0.2695
		(10.62; 1.6)	(32.72)	(4.03; 1.9)	(16.09)	(11.57; 1.9)	(27.63)	(6.77; 1.9)	(23.50)	(6.94; 2.2)	(20.07)	(2.47; 2.2)	(11.39)
	Algo	-0.0813		-0.0507		-0.0366		0.1681		-0.0445		-0.2073	
		(-2.21; 2.1)		(-1.26; 3.1)		(-0.61; 2.2)		(4.44; 3.2)		(-0.78; 2.7)		(-4.35; 4.2)	
	$\lvert$*Crowd*$\rvert$x*Algo*	0.0073	0.0225	0.0120		0.0051		0.0031		0.0032		0.0005	
		(3.25; 3.0)	(16.83)	(12.43; 3.0)		(10.16; 1.1)		(1.83; 1.1)		(9.73; 1.4)		(15.77; 1.0)	
	$\lvert$*Crowd*$\rvert$x*VPIN*	0.0105	0.0141	0.0242		0.0081		0.0022		0.0051		-0.0001	
		(14.00; 3.0)	(15.55)	(20.69; 3.0)		(10.42; 1.1)		(2.79; 1.1)		(2.15; 1.4)		(-1.14; 1.0)	
	Inst	-0.1568		-0.3321		-0.2384		-0.2079		-0.6724		-0.4103	
		(-0.71; 2.4)		(-1.15; 2.0)		(-0.97; 3.5)		(-0.82; 2.0)		(-1.75; 3.7)		(-1.05; 3.2)	
	C. Var.	0.0159	0.0159	0.0056		0.0016	0.0017	0.0001		0.0020	0.0019	0.0001	
		(88.53; 1.0)	(88.75)	(31.22; 1.0)		(19.69; 1.0)	(20.98)	(1.41; 1.0)		(5.70; 1.0)	(5.60)	(0.23; 1.0)	
	R^2	0.5716	0.3907	0.3492	0.2900	0.4514	0.3095	0.3735	0.2449	0.3839	0.1828	0.2582	0.1781
	Ind.	0.4929	(0.26; 0.95)	0.7452	(0.59; 0.79)	0.2250	(0.14; 0.35)	0.3534	(0.17; 0.73)	0.1065	(0.04; 0.12)	0.1714	(0.07; 0.29)
	$V \mid A$	0.3165	0.1764	0.5577	0.1875	0.1476	0.0774	0.2458	0.1076	0.0642	0.0322	0.0964	0.0731
		(0.16; 0.61)	(0.09; 0.34)	(0.45; 0.70)	(0.15; 0.23)	(0.09; 0.23)	(0.05; 0.12)	(0.12; 0.62)	(0.05; 0.36)	(0.02; 0.08)	(0.01; 0.04)	(0.02; 0.15)	(0.02; 0.18)

Figure 1. The anatomy of the 6 May 2010 flash crash

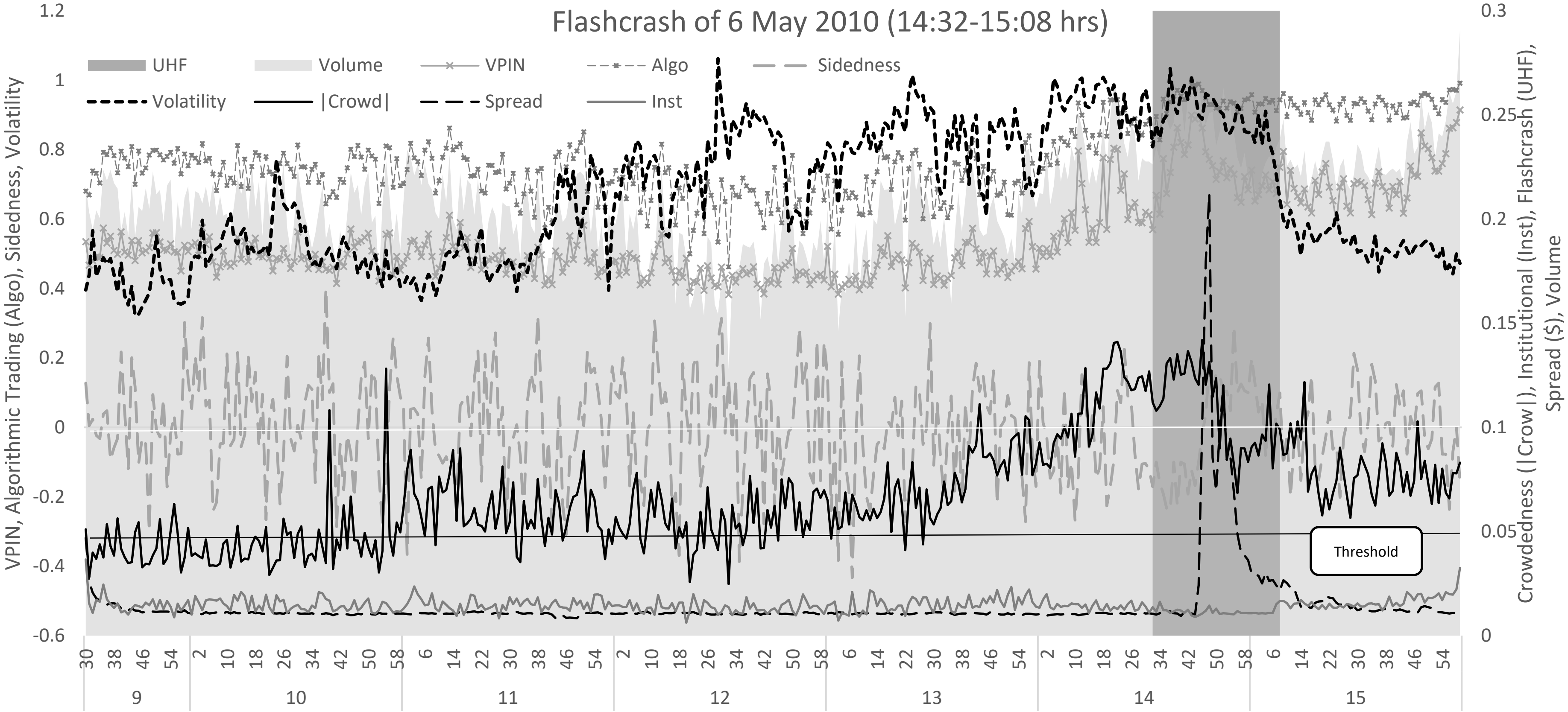

This figure plots nine microstructure measures during 6 May 2010. All observations are averages over one-minute intervals. In the legend, displayed at the top left of the figure: UHF is ultra-high frequency events, the light-grey shaded area is the log of aggregate volume (scaled by 1/10 for illustration purposes), VPIN is the percentage of trades that are informed, Algo is the percentage of trades that are algorithmic, Sidedness is the proportional trade imbalance, Volatility is the standard deviation of price change over the minute intervals, |Crowd| is our measure of crowdedness in $cents per unit of forecasting error in arbitrage capacity (SAC), Spread is the implied spread, and Inst. is the percentage of trades that are institutional. The vertical darker-shaded area is the officially reported duration of the flash crash. The horizontal black line shows the Crowd threshold for UHF events, estimated at 5 cents (right vertical axis). The horizontal white line is the 0 value of the left vertical axis.